# TOPICS IN NUCLEAR CHROMODYNAMICS:
## COLOR TRANSPARENCY AND HADRONIZATION IN THE NUCLEUS*

Stanley J. Brodsky

Stanford Linear Accelerator Center
Stanford University, Stanford, California 94309

## ABSTRACT

The nucleus plays two complimentary roles in quantum chromodynamics:

1. A nuclear target can be used as a control medium or background field to modify or probe quark and gluon subprocesses. Some novel examples are *color transparency*, the predicted transparency of the nucleus to hadrons participating in high momentum transfer exclusive reactions, and *formation zone phenomena*, the absence of hard, collinear, target-induced radiation by a quark or gluon interacting in a high momentum transfer inclusive reaction if its energy is large compared to a scale proportional to the length of the target. (Soft radiation and elastic initial state interactions in the nucleus still occur.) *Coalescence* with co-moving spectators is discussed as a mechanism which can lead to increased open charm hadroproduction, but which also suppresses forward charmonium production (relative to lepton pairs) in heavy ion collisions. I also discuss some novel features of nuclear diffractive amplitudes—high energy hadronic or electromagnetic reactions which leave the entire nucleus intact and give nonadditive contributions to the nuclear structure function at low $x_{Bj}$.

2. Conversely, the nucleus can be studied as a QCD structure. At short distances, nuclear wave functions and nuclear interactions necessarily involve *hidden color* degrees of freedom orthogonal to the channels described by the usual nucleon or isobar degrees of freedom. At asymptotic momentum transfer, the deuteron form

---

DISTI

factor and distribution amplitude are rigorously calculable.
One can also derive new types of testable scaling laws for
exclusive nuclear amplitudes in terms of the reduced am-
plitude formalism.

The lectures include a discussion of methods for computing wave
functions of hadrons, including new results for QCD in one-space
and one-time dimension using *discretized light-cone quantization*.
Tests of QCD in wave function-sensitive exclusive processes are
also reviewed. Explanations are proposed for two outstanding
anomalies in hadron phenomenology: the large spin-spin correla-
tion observed in large angle elastic proton-proton scattering, and
anomalous two-body hadronic decays of the $J/\psi$.

## I. INTRODUCTION

The least understood process in QCD is *hadronization* the mechanism
which converts quark and gluon quanta to color-singlet integrally-charged hadrons.
One way to study hadronization is to perturb the environment by introduc-
ing a nuclear medium surrounding the hard-scattering, short-distance reac-
tion. This is obviously impractical in the theoretically simplest processes
$e^+e^-$ or $\gamma\gamma$ annihilation. However, for large momentum transfer reactions oc-
curing in a nuclear target, such as deep inelastic lepton scattering or massive
lepton pair production, the nuclear medium provides a nontrivial perturbation to
jet evolution through the influence of initial and/or final state interactions. In
the case of large momentum transfer quasi-exclusive reactions, one can use a nu-
clear target to filter and influence the evolution and structure of the hadron wave
functions themselves. The physics of such nuclear reactions is surprisingly inter-
esting and subtle -involving concepts and novel effects quite orthogonal to usual
expectations.

The key to understanding hadronization and hadron matrix elements is the
hadron wave function itself. A convenient description of hadron wave functions is
given by the set of $n$-body momentum space amplitudes,

$$\psi_n(x_i, k_{\perp_i}, \lambda_i), \; i = 1, 2, \ldots n \; ,$$

defined on the free quark and gluon Fock basis at equal "light-cone time"
$\tau = t + z/c$ in the physical "light-cone" gauge $A^+ \equiv A^0 + A^3 = 0$. (Here
$x_i = k_i^+/p^+$, $\sum x_i = 1$, is the light-cone momentum fraction of quark or gluon

2

$i$ in the $n$-particle Fock state; $k_{\perp i}$, with $\sum k_{\perp i} = 0$, is its transverse momentum relative to the total momentum $p^\mu$; and $\lambda_i$ is its helicity.) The quark and gluon structure functions $G_{q/H}(x,Q)$ and $G_{g/H}(x,Q)$ which control hard inclusive reactions and the hadron distribution amplitudes $\phi_H(x,Q)$ which control hard exclusive reactions are simply related to these wave functions:

$$G_{q/H}(x,Q) = \sum_n \int^{Q^2} \Pi d^2 k_\perp \int \Pi dx_i \ |\psi_n(x_i,k_\perp)|^2 \delta(x_q - x) \ ,$$

and

$$\phi_H(x_i,Q) = \int^{Q^2} \Pi d^2 k_\perp \ \psi_{valence}(x_i,k_\perp) \ .$$

In the case of inclusive reactions all of the hadron Fock states generally participate; the necessity for higher-particle Fock states in the proton is apparent from its large gluon momentum fraction and the recent results from the EMC collaboration[1] suggesting that, on the average, little of the proton's helicity is carried by the light quarks.[2] In the case of high momentum transfer $Q$ exclusive reactions perturbative QCD predicts that only the lowest particle number (valence) Fock state contributes to leading order in $1/Q$. The essential gauge-invariant input is the distribution amplitude[3] $\phi_H(x,Q)$. Its dependence in $\log Q$ is controlled by evolution equations derivable from perturbation theory[3] or the operator product expansion.[4] A more detailed discussion of the light-cone Fock state wave functions and their relation to observables is given in Ref. 5.

The phenomenology of hadron wave functions in QCD is now just beginning. Constraints on the baryon and meson distribution amplitudes have been recently obtained using QCD sum rules and lattice gauge theory. The results are expressed in terms of gauge-invariant moments $<x_j^m> = \int \Pi dx_i \ x_j^m \ \phi(x_i,\mu)$ of the hadron's distribution amplitude. A "snapshot" of the proton's $uud$ wave function at equal light-cone time as deduced from QCD sum rules at $\mu \sim 1$ GeV by Chernyak et al.[6] is shown in Fig. 1. This will be discussed further in Sec. 7.

A new nonperturbative method "discretized light-cone quantization," (DLCQ)[7] has been developed which has the potential for providing detailed information on all the hadron's Fock light-cone components. The basic idea is to diagonalize the QCD Hamiltonian on the light-cone Fock states, using a computationally-convenient discrete momentum space basis. The eigenvalues $M^2$ of $H_{LC}$ provide the spectrum of the theory; the eigenvectors yield the Fock state
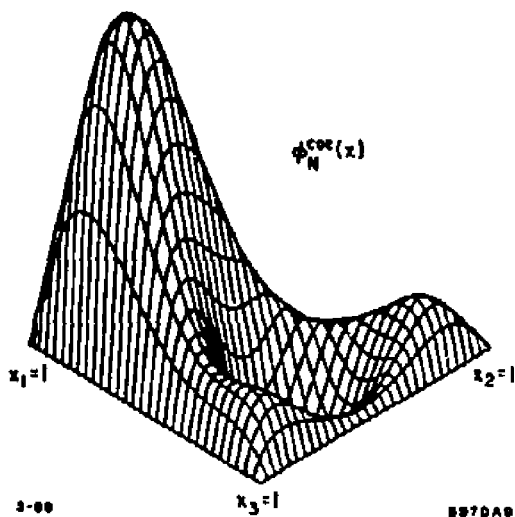
$\phi_N^{COR}(x)$

$x_1 = 1$

$x_2 = 1$

$x_3 = 1$

wave functions $\psi_n(x_i, k_{\perp_i}, \lambda_i)$. So far the method has been successfully applied to gauge theories and Yukawa theory (scalar gluons) in one-space and one-time dimension. New results for the spectrum and wave functions for QCD[1+1] are presented in Sec. 8.

The main emphasis of these lectures is the use of a nuclear target as a control medium or background field to modify or probe hadronization and quark and gluon subprocesses. I shall discuss several novel examples, including *color transparency*, the predicted diminished attenuation in the nucleus of hadrons participating in high momentum transfer *exclusive reactions*, and *formation zone phenomena*, the absence of hard collinear target-induced radiation by quarks or gluons interacting in a high momentum transfer *inclusive reactions*.

QCD factorization for hard inclusive processes implies, to leading order in $1/Q$, that the only nuclear dependence to the total production rate enters through the quark and gluon structure functions of the nucleus. This implies that initial and final state inelastic interactions inside the nucleus can be neglected in the high energy limit, contrary to usual intuition. This is the "formation zone" principle. Although inelastic initial and final state interactions can be neglected

4

for parton energies large compared to a scale set by the length of the target, soft radiation and elastic interactions are still effective and can lead to smearing of transverse momentum of the incoming and outgoing quarks and gluons.[8] The increased transverse momentum of the $\mu^+\mu^-$ pair measured by NA–SAVE–10[9] thus gives a measure[10] of the quark elastic cross section inside of nuclear matter. The total inclusive rate for lepton pair production is unchanged to leading order in $1/Q$. Further discussion, based on work[8] by Bodwin, Lepage and myself on the QCD target length condition is given in Sec. 5. It is remarkable that the incoming quark or antiquark can suffer *elastic* initial state interactions even though hard collinear *inelastic* interactions do not occur.

The target length condition and formation zone physics are important for the general understanding of the propagation of quark and gluon jets in nuclear matter. The converse of this effect is that particles produced at low velocities relative to other hadrons, including the beam spectators, will have their momentum strongly distorted by final state interactions. For example, the "coalescence" of the heavy quarks with beam spectators can cause severe distortions of the momentum distribution of heavy hadrons produced in the beam direction, although the total inclusive rate for heavy quark production is unchanged to leading order in $1/M_Q$. Gunion, Soper and I[11] note that this effect may account for some of the anomalies observed in charm hadroproduction experiments, such as the large cross section for charmed-strange baryon production at large $x_L$ by a 135 GeV/$c$ hyperon beam measured by the WA–42 collaboration[12] at the SPS, the large cross sections recently reported by the E–400 group at Fermilab for open charm hadron production by high energy neutron beams, as well as the ISR results for $\Lambda_c$ production in $pp$ collisions. The coalescence effect may be modified by the nuclear environment which could in turn cause an $x_L$-dependence of the production rate for charmed hadrons in nuclear targets. Most interesting, the inclusive production of quarkonium states can be strongly affected by the presence of co-movers. In fact, Mueller and I[13] that due to coalescence of the $c$ or $\bar{c}$ quark with beam spectators, one expects a depletion at low transverse momentum of $J/\psi$ production by a nuclear beam relative to continuum lepton pair production. The coalescence effect occurs independent of whether or not a quark-gluon plasma is formed. Further discussion will be given in Sec. 4.

It is helpful to review the basic time scales involved in hadronization. For processes involving hard interactions, it is convenient to consider two separate time

scales, a time of production $\tau_P$, and a time for formation of the measured final state hadron $\tau_F$. We define these times in the laboratory system where the target nucleon or nucleus is at rest. $\tau_P$ is the time scale over which the interaction occurs, while $\tau_F$ is the time it takes the produced partonic system to reach the normal configuration of the wave function of the hadron. If there is no hard interaction the distinction between $\tau_P$ and $\tau_F$ is lost. For processes involving a hard collision, and at times after the collision less than $\tau_F$, one must deal with the partonic system explicitly. Indeed, it is only after a time $\tau_F$ that it makes sense to talk of a particular hadron as existing.

For a process involving a hard momentum transfer $Q$ (or production of a heavy quark system), we can, following Bjorken and Mueller,[4] estimate $\tau_P \sim 1/\Delta E \sim p/Q^2$ where $p$ is the momentum of relativistic hadron $H$. The time of formation of $H$ is determined by requiring that $v_\perp \tau_F = r_H$ where $v_\perp$ is the transverse velocity of a quark constituent of $H$ and $r_H$ is the radius of the hadron. Now $v_\perp = \sqrt{(2/3)}k_H/E_H$ where $k_H$ is the typical momentum of the constituent in the rest system of $H$, and $E_H$ is the laboratory energy of $H$. Thus $\tau_F \sim (r_H/k_H)E_H$, and at high energies the formation time is typically much longer than the production time. For processes involving only soft collisions, the distinction between $\tau_P$ and $\tau_F$ is lost.

In general, the $A$-dependence of the cross section for producing a relativistic hadron $H$ depends on three factors: (i) the interaction of the initial projectile with upstream nucleons in the nucleus before the hard collision; (ii) the interaction of the partonic constituents of $H$ with the nucleus or, if $\tau_F$ is small enough, the interaction of $H$ itself with the nucleus; (iii) the interaction of the partonic constituents of $H$ with other quarks and gluons, co-moving with the $H$-system, during times less than $\tau_F$. For example, the fact that the $J/\psi$ is typically formed far outside of a nucleus at high energy implies that the hadronic cross sections deduced for the $J/\psi$ nucleon cross section from the relatively low nuclear final state corrections are incorrect.[5] This is discussed in more detail in Sec. 2.[16]

Nuclear effects predicted by perturbative QCD are even more exotic for hard exclusive processes. Only the valence Fock component of a hadron's wave function with small transverse size of order $1/Q$ contributes to an exclusive amplitude at high momentum transfer in QCD. Such a wave function component has only a small color dipole moment and thus has a strong interaction cross section of

order $1/Q^2$. This implies that a hadron can hard scatter on every nucleon in a nucleus without attenuation from initial or final state interactions! In contrast to inclusive hard reactions, even elastic scattering initial and final state interactions are negligible. Because of the formation zone effect the hadronic state stays small over a distance which grows with its energy. The prediction that the rate for quasi-elastic hard scattering exclusive processes will be additive on the number of nucleons in the nucleus at large momentum transfer and hadron energy is referred to as "color transparency."[16] A crucial experiment is quasi-elastic lepton-proton scattering in the nucleus—QCD predicts a monotonic rise in the transparency ratio as the momentum transfer is raised until complete additivity is reached. The energy dependence of the formation zone effect can be isolated by studying final state attenuation as a function of recoil proton energy at a given momentum transfer $Q^2$.

A test of QCD color transparency has recently been carried out at BNL in large momentum transfer quasi-elastic $pp$ scattering at $\theta_{cm} \simeq \pi/2$ in several nuclear targets (C, Al, Pb) by a BNL–Columbia–Penn State collaboration.[17] A schematic of this process is shown in Fig. 2. The attenuation of the recoil proton as it traverses the nucleus and its momentum distribution $dN/dp_y$ transverse to the $x$–$z$ scattering plane are measured.
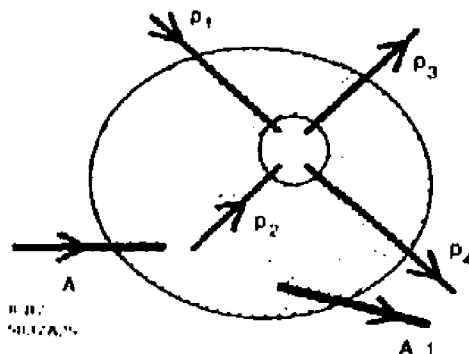


Fig. 2. Quasi-elastic $pp$ scattering inside a nuclear target. In conventional Glauber theory, this process is attenuated by the elastic and inelastic interactions of the incident proton and the final state interactions of the scattered and recoil protons.

The results are rather astonishing. As shown in Fig. 3, the quasi-elastic cross section is strongly attenuated at low $p_{lab} \sim 6$ GeV/c consistent with conven-
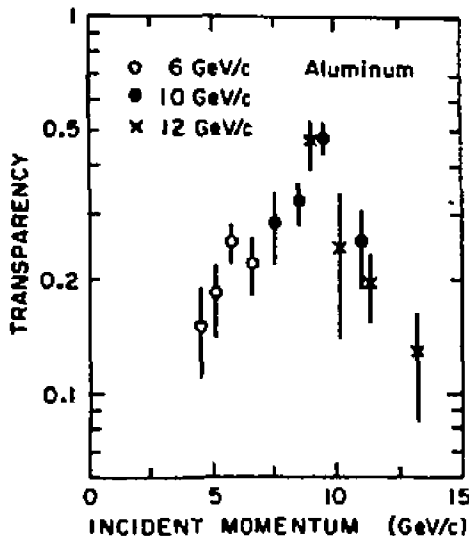
Fig. 3. Measurements of the transparency ratio

$$T = \frac{d\sigma}{dt}[pA \to pp(A-1)]/Z\frac{d\sigma}{dt}(pp \to pp)$$

near 90° on Aluminum (Ref. 17). Conventional Glauber theory predicts that this ratio should be constant in energy. Perturbative QCD predicts a monotonic rise.

tional Glauber initial and final state absorption. As $p_{lab}$ is increased the attenuation decreases rapidly as predicted by perturbative QCD. This appears to support the color transparency prediction. However, beyond $p_{lab} = 10$ GeV/c the rate falls dramatically; at $p_{lab} = 12$ GeV/c, normal attenuation is observed, in contradiction to the expectation from perturbative QCD that the transparency effect should become even more apparent! Thus, neither conventional nuclear physics nor leading twist perturbative QCD can explain the data. However, we note that the spin-spin correlation, $A_{NN}$, also has a dramatic anomaly at $p_{lab} = 11.75$ GeV/c (see Fig. 4). de Teramond and I[18] have attempted (see Sec. 9) to explain the origin of both phenomena in terms of the onset of new degrees of freedom, i.e., a resonance or threshold enhancement in the dibaryon system at $\sqrt{s} \sim 5$ GeV, possibly associated with the onset of charmed hadron production. Color transparency fails at a resonance since the full Fock structure of the proton is involved.[18]
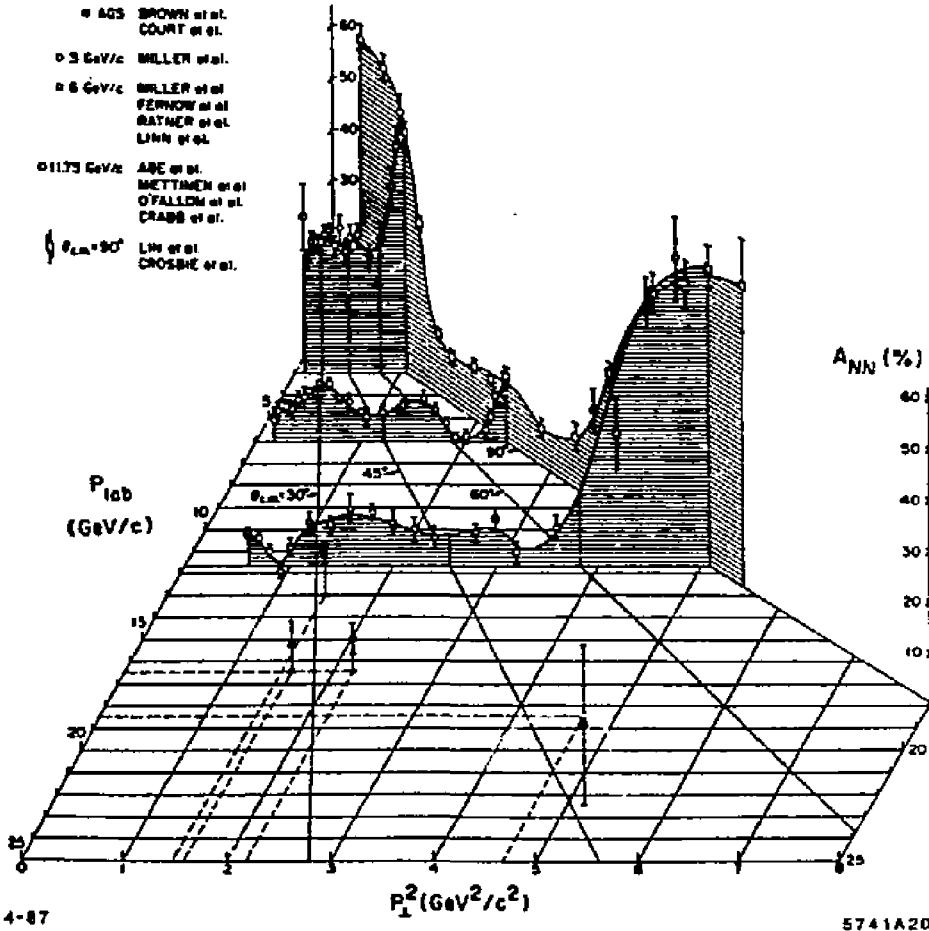
8

Fig. 4. The spin-spin correlation $A_{NN}$ for elastic $pp$ scattering with beam and target protons polarized normal to the scattering plane (Ref. 19). $A_{NN} = 60\%$ implies that it is four times more probable for the protons to scatter with spins parallel rather than antiparallel.

Another very important test of these novel QCD considerations is $\bar{p}p \rightarrow J/\psi$ production deep inside of a nucleus. Again, color transparency implies negligible initial state attenuation of the incoming antiproton in striking contrast to conventional nuclear physics expectations. We discuss this interesting process[20] in more detail in Sec. 3.

The nucleus itself must be described as a QCD structure. At short distances, nuclear wave functions and nuclear interactions necessarily involve *hidden color*, degrees of freedom orthogonal to the channels described by the usual nucleon or isobar degrees of freedom. In the case of the deuteron, five color-singlet Fock states are required just to describe its six-quark valence wave function. At asymptotic momentum transfer, the deuteron form factor and distribution amplitude are rigorously calculable. At subasymptotic momenta, one can derive new types of scaling laws for exclusive nuclear amplitudes in terms of the reduced amplitude formalism. A brief review is given in Secs. 10 and 11.

I also briefly discuss in Sec. 6 some novel features of *nuclear diffractive* amplitudes—high energy hadronic or electromagnetic reactions which leave the entire nucleus intact. In the case of deep inelastic scattering, such leading twist contributions can give unusual nonadditive contributions to the nuclear structure function at low $x_{Bj}$. In the case of vector meson electroproduction at highly virtual photon mass, diffractive processes can give essential information on nonforward matrix elements of the same operator products which control deep inelastic lepton scattering.[21]

I also will briefly review of the status of QCD predictions for exclusive processes involving large momentum transfer (see Sec. 7). There are still questions regarding the magnitude of the momentum transfer required for the validity of the leading order predictions. The experimental observation of "color transparency" in *pp* quasi-elastic scattering helps to establish the basic validity of the predictions in the experimentally accessible domain. It is thus even more important to understand experimental anomalies, and I discuss two important topics in Secs. 9 and 12: the surprisingly strong spin-spin correlations in elastic *pp* scattering and the unusual descrepancy between the decays of the $J/\psi$ and $\psi'$ into pseudoscalar/vector hadronic decays. Both phenomena can be understood as effects due to new $S$ channel thresholds.

The application of QCD to nuclei- *Nuclear Chromodynamics* has brought together two formerly distinct communities of physicists. Given that the natural scale of QCD is 1 fermi, nuclear physics can hardly be studied as an isolated subject, divorced from nucleon substructure. Indeed, several traditional assumptions of nuclear theory are incompatible with QCD, such as (a) standard on-shell form factor factorization in impulse approximation and (b) Dirac equation phenomenology for nucleon interactions in nuclei since the $N N \overline{N}$ intermediate state

is severely suppressed by nucleon compositeness.[22] Conversely, the most difficult questions for particle theorists—the structure of the hadrons in terms of their quark and gluon degrees of freedom, gluonium and other exotic spectra, coherence effects, jet hadronization and particle formation, the nature of the pomeron, diffractive and forward processes, etc., require experimental input at all energy scales, including the regime of tens of GeV or even lower.

## 2.    INCLUSIVE $J/\psi$ PRODUCTION IN NUCLEI

The production of heavy quarkonium states such as the $J/\psi$ in collisions involving nuclei can test many of the fundamental features of QCD outlined in the introduction. The simplifying feature of such reactions is that the underlying production subprocess involves heavy quark pair production at small transverse distances $r_\perp \lesssim 1/M_Q$. Mueller and I[13] have analyzed the nuclear dependence of a number of processes ranging from quasi-elastic $\bar{p}p \to J/\psi$ production in nuclear reactions to quasi-exclusive and inclusive photoproduction reactions, to fully inclusive $J/\psi$ production in nucleus-nucleus collisions. The latter process has become especially interesting recently because of the suggestion[23] that the attenuation of $J/\psi$ production in ion-ion collisions relative to the lepton-pair background might provide a signal for quark-gluon plasma formation. We will show here that such attenuation is a natural feature of inclusive nucleon reactions independent of the state of nuclear matter. We also show that the cross section $\sigma(J/\psi, N)$ for $J/\psi$ scattering on nucleons cannot be directly determined from high energy photoproduction reactions.
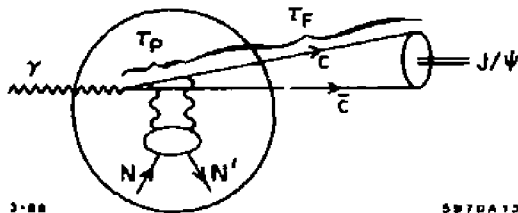


Fig. 5.  Schematic representation of charmonium photoproduction in a nuclear target.

We begin with a description of quasi-elastic $J/\psi$ photoproduction in a nucleus (see Fig. 5). (We assume that the momentum transfer is sufficient that

coherent production to nucleons can be neglected.) To leading order in $1/M_Q$, the photon couples directly to the heavy quark. As discussed in the introduction, the production time for the $c\bar{c}$ system (in the target rest frame) is quite short:

$$\tau_{\text{prod}} \simeq \frac{1}{M_Q} \frac{p_\gamma}{M_Q} \sim 10 \text{ GeV}^{-1} = 2 \text{ fm}$$

at $p_\gamma \sim 100$ GeV. The formation time required for the $c\bar{c}$ to separate to a transverse size comparable to the radius of the $J/\psi$ is

$$\tau_{\text{formation}} \simeq \frac{r_{J/\psi}}{v_\perp} \sim \frac{\frac{1}{2} \text{fm}}{\frac{1}{2} \text{ GeV}/p_\gamma} \sim 1 \text{ fm } p_\gamma \text{ (GeV)} .$$

Thus, even at $p_\gamma \sim 10$ GeV the $J/\psi$ state is produced far from the nucleus. Since the $c\bar{c}$ system remains a small color singlet as it transverse the nucleus, we expect negligible initial or final state interactions, aside from EMC-type nonadditive distributions of the structure functions. One thus predicts

$$A_{\text{eff}} = \frac{\sigma(\gamma A \to J/\psi A^*)}{\sigma(\gamma N \to J/\psi N^*)} \simeq A .$$

Let us contrast this result with the conventional eikonal analysis. There one uses formulae of the form $[\eta = \eta(\rho, z)$ is the nuclear density]

$$A_{\text{eff}} = \int\limits_0^R 2\pi \rho \, d\rho \int\limits_{-\sqrt{R^2-\rho^2}}^{\sqrt{R^2-\rho^2}} dz \, \eta \, e^{-\sigma(\sqrt{R^2-\rho^2}+z)\eta} ,$$

corresponding to the $J/\psi$ being created at impact distance $\rho$ and longitudinal coordinate $z$ with respect to the center of the nucleus. This formulation assumes that the $J/\psi$ is produced as a physical particle immediately after creation of the $c\bar{c}$ pair. In fact, the formation time is so long that what passes through the nucleus is *not* a normal $J/\psi$, and hence the effective cross section $\sigma$ extracted using (3.1) has little to do with $J/\psi$ scattering on a nucleon. Thus present photoproduction experiments have not determined the physical $J/\psi$ nucleon cross section. $J/\psi$ photoproduction experiments from both SLAC ($E_\gamma \sim 10$ GeV) and Fermilab ($E_\gamma \sim 200$ GeV) (E691 and E537) find $A_{\text{eff}} \sim A^{0.95}$ close to but below complete additivity. In the low energy SLAC experiment, the $c\bar{c}$ may separate enough to provide some attenuation. In the high energy Fermilab experiment the transverse separation of the $c$ and $\bar{c}$ should remain small during passage through the nucleus.

## 3. COLOR TRANSPARENCY AND QUASI-EXCLUSIVE $J/\psi$ PRODUCTION IN $\bar{p}A$ COLLISIONS

Novel features of QCD, including color transparency, can be studied by measuring quasi-exclusive $J/\psi$ production by antiprotons in a nuclear target. We are particularly interested in the quasi-exclusive annihilation process $\bar{p}A \to J/\psi(A-1)$ where the nucleus is left in a ground or excited state, but extra hadrons are not created (see Fig. 6). The cross section involves a convolution of the $\bar{p}p \to J/\psi$ subprocess cross section with the distribution $G_{p/A}(y)$ where $y = (p^0+p^3)/(p_A^0+p_A^3)$ is the boost-invariant light-cone fraction for protons in the nucleus. This distribution can be determined from quasi-exclusive lepton-nucleon scattering $\ell A \to \ell p(A-1)$.
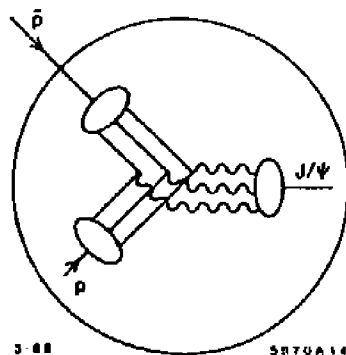
Fig. 6. Schematic representation of quasi-elastic charmonium production in $\bar{p}A$ reactions.

In first approximation $\bar{p}p \to J/\psi$ involves $qqq + \bar{q}\bar{q}\bar{q}$ annihilation into three charmed quarks. The transverse momentum integrations are controlled by the charm mass scale and thus only the Fock state of the incident antiproton which contains three antiquarks at small impact separation can annihilate. Since this state has a relatively small color dipole moment it should have a longer than usual mean-free path in nuclear matter, i.e., "color transparency." Thus, unlike traditional expectations, QCD predicts that the $\bar{p}p$ annihilation into charmonium is not restricted to the front surface of the nucleus. The exact nuclear dependence also depends on the formation time for the physical $\bar{p}$ to couple to the small $\bar{q}\bar{q}\bar{q}$ configuration, $\tau_F \sim \frac{\tau_p}{k_r} E_p$. It may be possible to study the effect of finite formation

13

time by varying the beam energy, $E_p$, and using the Fermi-motion of the nucleon to stay at the $J/\psi$ resonance.

Since the $J/\psi$ is produced at nonrelativistic velocities in this low energy experiment, it is formed inside the nucleus. The $A$-dependence of the quasi-exclusive reaction can thus be used to determine the $J/\psi$–nucleon cross section at low energies. For a normal hadronic reaction $\bar{p}A \to HX$, we expect $A_{eff} \sim A^{1/3}$, corresponding to absorption in the initial and final state. In the case of $\bar{p}A \to J/\psi X$ we expect $A_{eff}$ much closer to $A^1$ if color transparency is fully effective and $\sigma(J/\psi N)$ is small.

## 4.    COALESCENCE AND THE EFFECT OF CO-MOVERS

What happens if two jets overlap in phase-space? Certainly independent fragmentation of the jets will fail because of coherent effects. In QED there are strong final state interactions when two charged particles are produced at low relative velocity. In the case of particles of opposite charge, the QED Born cross sections are corrected by the factor:[24]

$$\sigma = \sigma_0 \frac{2\pi Z_1 Z_2 \alpha/v}{1 - \exp(-2\pi Z_1 Z_2 \alpha/v)} \ ,$$

which increases the cross section dramatically at low relative velocity $v$. We expect similar effects in QCD when two jets can coalesce to attractive color channels ($Z_1 Z_2 \alpha \to C_F \alpha_s$ for $q\bar{q}$ color singlets). In the case of electroproduction, the low relative velocity enhancements provide a simple estimate of the increase of the $ep \to eX$ cross section at low values of $W^2 = (q + p)^2$, beyond that given by simple duality arguments.

Strong final state interaction effects occur most strongly when particles have low relative velocity and thus minimum invariant mass. Kinematically, the invariant mass $\mathcal{M}^2$ of a set of particles $i = 1 \ldots n$ with total momentum $P^\mu$ is given by

$$\frac{\mathcal{M}^2 + \vec{P}_\perp^2}{P^+} = \sum_{i=1}^{n} \frac{m_i^2 + \vec{k}_{\perp i}^2}{k_i^+} \ , \quad \Sigma \vec{k}_\perp = \vec{P}_\perp \ , \quad \Sigma k^+ = P^+ \ .$$

This is minimized for $(m_\perp^2 \equiv \vec{k}_\perp^2 + m^2)$

$$x_i \equiv \frac{k_i^+}{P^+} = \frac{m_{\perp i}}{\sum_{j=1}^{n} m_{\perp j}} \ ,$$

14

which corresponds to particles produced at equal rapidity. Thus, a light quark will interact strongly with a heavy quark if $x_q/x_Q \sim m_{\perp q}/m_{\perp Q}$.

Gunion, Soper and I[11] have recently proposed the coalescence mechanism as an explanation of the observed leading particle correlations seen in charm hadroproduction experiments and the anomalously large cross section[12] observed at the SPS for $\Sigma^- N \rightarrow A^+(csu)X$ at large $x_L$. [The hyperon momentum was 135 GeV/c.] The correction to the rate, integrated over relative rapidity, vanishes just as a single inverse power of the heavy quark mass, and thus may give significant corrections to charm production rates and distributions.

According to perturbative QCD, the inclusive production of heavy quarks can be computed to leading order in $1/m_Q$ from the fusion processes $gg \rightarrow Q\overline{Q}$ and $q\bar{q} \rightarrow Q\overline{Q}$ and the corresponding quark and gluon structure functions. In addition, especially in the case of charm, there are possibly important contributions to the heavy quark structure function of the proton $G_{Q/p}(x,Q)$ and heavy quark hadroproduction at large $x_L$ or large $x_B$, due to scattering from "intrinsic" heavy quark Fock states containing $QQ$ pairs in the wave function (see Fig. 7). However, for very heavy quarks, such contributions are suppressed by relative factors of $1/m_Q^2$.
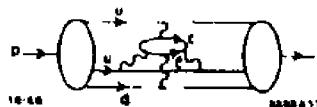


Fig. 7. Example of an intrinsic $qqq\bar{c}c$ Fock state in the proton.

According to QCD factorization, all effects due to final state interactions are unitary and thus cannot affect the total heavy quark production rate to leading order in $1/m_Q$. Nevertheless, when the heavy quark is produced in the beam direction it can interact strongly with co-moving quarks or gluons; for example, the forward-moving spectator partons of the beam hadron or nucleus which have nearly the same velocity as the produced $Q$ or $\overline{Q}$. Thus, the interactions with the co-moving spectators can strongly modify the local momentum distribution of the $Q$ or $\overline{Q}$ relative to the tree-graph calculation, increasing the production at large $x_L$ relative to lower momenta. This is illustrated for hyperon production of a

charmed-strange baryon in Fig. 8. In the Coulomb interaction model calculated by Gunion, Soper and myself, all of these features were observed, and the integrated rate was unchanged up to terms of order $1/m_Q$.
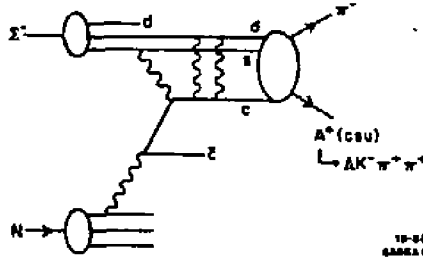


Fig. 8. Illustration of the coalescence of a charmed quark with beam spectator quarks in the process $\Sigma^- N \to A^+(csu)X$. The final state interactions represented by gluon exchange can lead to a strong distortion of the charmed hadron momentum distribution toward large $x_L$ relative to the gluon-gluon fusion Born approximation prediction.


The interactions of the produced $Q$ and $\overline{Q}$ with co-moving hadrons can clearly have a severe effect on the production of individual heavy quark states at low $p_T$. For example, the coalescence of the charm quark with beam spectators can increase the production rate of $c\bar{q}$ or $cqq$ states at the expense of $c\bar{c}$ formation. Thus the forward production of $J/\psi$ will be strongly depleted in central nuclear collisions (high transverse energy) relative to continuum lepton pair production because of the increased density of co-moving partons from the beam.[13] As the transverse momentum of the $J/\psi$ is increased the depletion is predicted to disappear. In contrast to predictions based on the existence of a quark-gluon plasma, this depletion occurs independent of whether the target is a light or heavy nucleus! We thus urge that ion beam experiments be carried out on hydrogen or light nuclei where a plasma is not expected to be formed.

The Sommerfeld factor also can be used to estimate the behavior of exclusive amplitudes near threshold. For example, the production of meson pairs in two-photon annihilation can be modeled[25] by calculating the differential cross section in QCD tree graph approximation and then multiplying by the QCD version of the Sommerfeld factor appropriate to the relative velocity of the respective quark pair.

## 5. FORMATION ZONE PHENOMENA IN DEEP INELASTIC SCATTERING

One of the remarkable consequences of QCD factorization for inclusive reactions at large $p_T$ is the absence of inelastic initial or final state interactions of the high energy particles in a nuclear target. Since structure functions measured in deep inelastic lepton scattering are essentially additive (up to the EMC deviations), factorization implies that the $q\bar{q} \to \mu^+\mu^-$ subprocesses in Drell–Yan reactions occurs with equal probability on each nucleon throughout the nucleus. At first sight this seems surprising since one expects energy loss from inelastic initial state interactions.
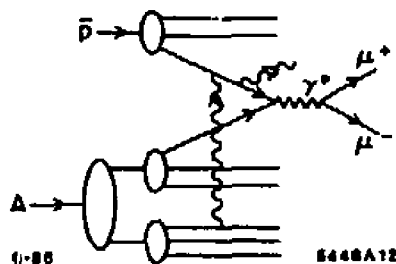


Fig. 9. Induced radiation from the propagation of an antiquark through a nuclear target in massive lepton production. Such inelastic interactions are coherently suppressed at parton energies large compared to a scale proportional to the length of the target.

In fact, inelastic reactions such as hard gluon bremsstrahlung induced in the nucleus which could potentially decrease the incident parton energy (illustrated in Fig. 9) are suppressed by coherence if the quark energy (in the laboratory frame) is large compared to the target length:

$$E_q > \mu^2 \, L_A \ .$$

Here $\mu^2$ is the difference of mass squared between the incident quark and the quark-gluon pair produced in the initial or final state collision. This phenomenon has its origin in studies of QED processes by Landau and Pomeranchuk. The QCD analysis is given by Bodwin, Lepage and myself.[8] The result can be derived by showing that the hard inelastic radiation emitted from differing scattering centers destructively interferes provided the target length condition is maintained.

17

The destuctive interference occurs when the momentum transfer $\mu^2/E_q$ due to the induced radiation is smaller than the inverse of the separation between two scattering centers in the nucleus. Soft radiation and elastic collisions, however, are still allowed, so one predicts collision broadening of the initial parton transverse momentum. Recent measurements of the Drell–Yan process $\pi A \to \mu^+\mu^- X$ by the NA-10 group[26] at the CERN–SPS confirm that the cross section for muon pairs at large transverse momentum is increased in a tungsten target relative to a deuteron target (see Fig. 10). Since the total cross section for lepton-pair production scales linearly with $A$ (aside from relatively small EMC-effect corrections), there must be a corresponding decrease of the ratio of the differential cross section at low values of the di-lepton transverse momentum. This is also apparent in the data.
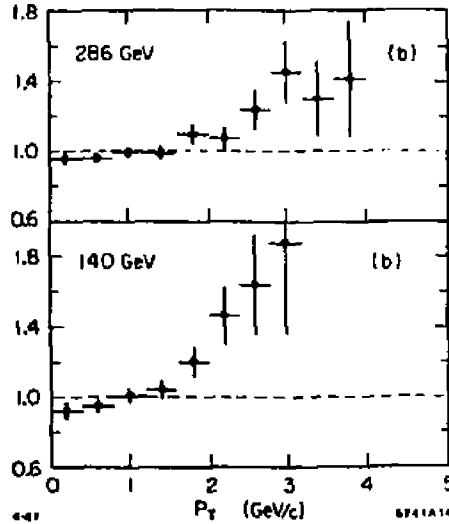


Fig. 10. The ratio $\sigma(\pi^- W \to \mu^+\mu^- X)/\sigma(\pi^- D \to \mu^+\mu^- X)$ as a function of the pair transverse momentum (Ref. 26).

These results have striking implications for the interaction of the recoil quark jet in deep inelastic electron-nucleus scattering. For the quark (and gluons) satisfying the length condition, there should be no extra radiation induced as the parton traverses the nucleus. However, low energy gluons, emitted in the deep inelastic electron-quark collision, can suffer radiative losses, leading to cascading

of soft particles in the nucleus. It is clearly very important to study this phenomena as a function of recoil quark energy and nuclear size. It should be emphasized that the absence of inelastic initial or final state collisions for high energy partons does not preclude collision broadening due to elastic initial or final state interactions. The elastic corrections are unitary to leading order in $1/Q$ and do not affect the normalization of the deep inelastic cross section. Thus one predicts that the mean square transverse momentum of the recoil quark and its leading particles will increase as $A^{1/3}$.

The transverse momentum of the recoil quark reflects the intrinsic transverse momentum of the nucleon wave function. The EMC effect[27] implies that quarks in a nucleus have smaller average longitudinal momentum than in a nucleon.[28] Independent of the specific physical mechanism underlying the EMC effect,[28] the quarks in a nucleus would also be expected to have smaller transverse momentum. This effect can counteract to a certain extent the collision broadening of the outgoing jet.

Unlike the struck quark the remnant of the target system does not evolve with the probe momentum $Q$. However, the quantum numbers of the spectator system is $\bar{3}$ in color, so nonperturbative hadronization must occur. Since the transverse momentum of the leading particles in the spectator jet is not affected by the QCD radiative corrections, it more closely reflects the intrinsic transverse momentum of the hadron state.

It is also interesting to study the behavior of the transverse momentum of the quark and spectator jets as a function of $x_{B_j}$. For $x_{B_j} \sim 1$, the 3-quark Fock state dominates the reaction. If the valence state has a smaller transverse size[3] than that of the nucleon, averaged over all of its Fock components, then one expects an increase of $\langle k_\perp^2 \rangle$ in that regime. Evidence for a significant increase of $\langle k_\perp^2 \rangle$ in the projectile fragmentation region at large quark momentum fractions has been reported by the SFM group[29] at the ISR for $pp \to$ di-jet $+X$ reactions.

## 6.  DIFFRACTION CHANNELS AND NUCLEAR STRUCTURE FUNCTION NONADDITIVITY

One unusual source of nonadditivity in nuclear structure functions (EMC effect) are electroproduction events at large $Q^2$ and low $x$ which nevertheless leave the nucleus completely intact $x < (1/M_N L_A)$, where $L_A$ is the target length. In the

case of QED, analogous processes such as $\gamma^* A \to \mu^+ \mu^- X$ yield nuclear-coherent contributions which scale as $A_{eff} = Z^2/A$ [see Fig. 11(a)]. Such Bethe-Heitler processes contribute to the Bjorken-scaling, leading-twist cross section.[3b] In QCD we expect[31] the nuclear dependence to be less than additive $A_{eff} \sim A^{2/3}$ for the analogous gluon exchange contributions [see Fig. 11(b)] because of their diffractive coupling to the nucleus. One can identify nuclear-coherent event contributions by observing a rapidity gap between the produced particles and the recoiling target. An interesting question is how the gluon momentum fraction sum rule for the total nucleus is modified by the diffractive contributions.
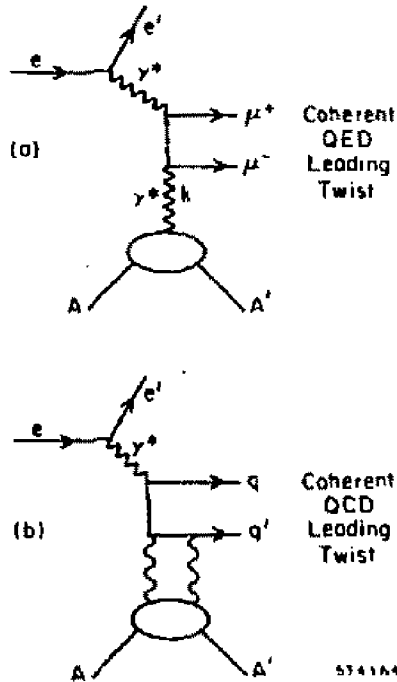


Fig. 11. Leading twist contributions to deep inelastic lepton-nucleus scattering that leave the target intact: (a) QED example, (b) QCD example.

20

## 7.   EXCLUSIVE PROCESSES IN QCD

There has been significant progress in the theoretical development of QCD in the past few years. This includes the extension of factorization and evolution equations to the domain of exclusive hadronic and nuclear amplitudes. In high momentum transfer inclusive reactions, the underlying quark and gluon scattering processes lead directly to jet production in the final state. To leading order in $1/Q^2$, the cross sections and jet hadronization can be understood at the probabilistic level. In contrast, in *exclusive* electroproduction processes, one studies quark and gluon scattering and their reformation into hadrons at the *amplitude* level. Exclusive reactions thus depend in detail on the composition of the hadron wave functions themselves. Moreover, QCD sum rule techniques have made tantalizing predictions for the required hadron wave functions, results which are being confirmed by lattice gauge theory computations.

There is now an extensive literature, both experimental and theoretical, describing the features of large momentum transfer exclusive reactions. The QCD predictions are based on a factorization theorem[3,4] which separates the nonperturbative physics of the hadron bound states from the hard scattering amplitude which controls the scattering of the constituent quarks and gluons from the initial to final directions. This factorization is illustrated for the proton form factor in Fig. 12. The application to the deuteron form factor is presented in Sec. 10.

Electroproduction of exclusive channels provides one of the most valuable testing grounds of this QCD formalism, since the incoming photon provides a probe of variable space-like mass directly coupling to the hard-scattering amplitude.

It has been known since 1970 that a theory with underlying scale-invariant quark-quark interactions leads to dimensional counting rules[32] for large momentum transfer exclusive processes, e.g., $F(Q^2) \sim (Q^2)^{1-n}$ where $n$ is the minimum number of quark fields in the hadron. QCD is such a theory; the factorization formula leads to nucleon form factors of the form:[33]

$$G_M(Q^2) = \left[\frac{\alpha_s(Q^2)}{Q^2}\right]^2 \sum_{n,m} a_{nm} \left(\ln \frac{Q^2}{\Lambda^2}\right)^{-\gamma_n - \gamma_m}$$

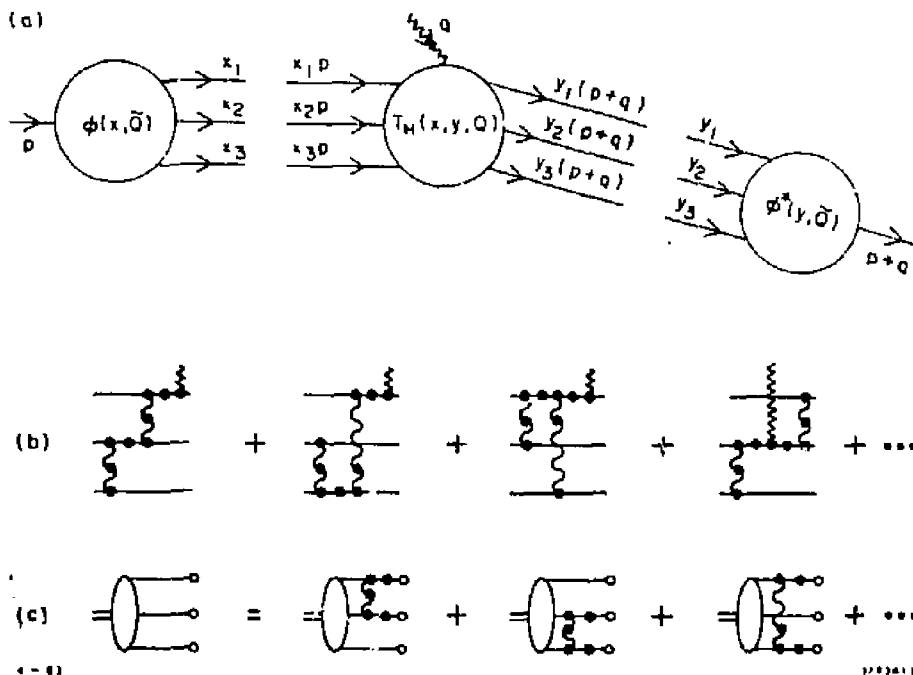$$\times \left[1 + \mathcal{O}(\alpha_s(Q)) + \mathcal{O}\left(\frac{1}{Q}\right)\right].$$

Fig. 12. (a) Factorization of the nucleon form factor at large $Q^2$ in QCD. (b) The leading order diagrams for the hard scattering amplitude $T_H$. The dots indicate insertions which enter the renormalization of the coupling constant. (c) The leading order diagrams which determine the $Q^2$ dependence of the distribution amplitude $\phi(x, Q)$ defined in Sec. 1.

The first factor, in agreement with the quark counting rule, is due to the hard scattering of the three valence quarks from the initial to final nucleon direction. Higher Fock states lead to form factor contributions of successively higher order in $1/Q^2$. The logarithmic corrections derive from an evolution equation[3,33] for the nucleon distribution amplitude. The $\gamma_n$ are the computed anomalous dimensions, reflecting the short distance scaling of three-quark composite operators. The results hold for any baryon to baryon vector or axial vector transition amplitude that conserves the baryon helicity. Helicity nonconserving form factors should fall as an additional power of $1/Q^2$. Measurements of the transition form factor to the $J = 3/2$ $N(1520)$ nucleon resonance are consistent with $J_z = \pm 1/2$ dominance, as predicted by the helicity conservation rule.[34] A review of the data on spin effects in electron nucleon scattering in the resonance region is given in Ref. 35. It

22

is important to explicitly verify that $F_2(Q^2)/F_1(Q^2)$ decreases at large $Q^2$. The angular distribution decay of the $J/\psi \to p\bar{p}$ is consistent with the QCD prediction $\lambda_p + \lambda_{\bar{p}} = 0$.

The normalization constants $a_{nm}$ in the QCD prediction for $G_M$ can be evaluated from moments of the nucleon's distribution amplitude $\phi(x_i, Q)$. There are extensive ongoing theoretical efforts computing constraints on this nonperturbative input directly from QCD. The pioneering QCD sum rule analysis of Chernyak and Zhitnitskii[36] provides constraints on the first few moments of $\phi(x, Q)$. Using as a basis the polynomials which are eigenstates of the nucleon evolution equation, one gets a model representation of the nucleon distribution amplitude, as well as its evolution with the momentum transfer scale. A pictorial representation of the most recent results for the proton's distribution amplitude is given in Fig. 1.

The QCD sum rule analysis predicts a surprising feature: strong flavor asymmetry in the nucleon's momentum distribution. The computed moments of the distribution amplitude imply that 65% of the proton's momentum in its 3-quark valence state is carried by the u-quark which has the same helicity as the parent hadron. A recent comprehensive reanalysis by King and Sachrajda[37] has now confirmed the Chernyak and Zhitnitskii form in its essential details.

Dziembowski and Mankiewicz[38] have recently shown that the asymmetric form of the CZ distribution amplitude can effectively be derived from a rotationally-invariant center-of-mass wave function transformed to the light cone using a Melosh-type boost of the quark spinors. The transverse size of the valence wave function is found to be significantly smaller than the mean radius of the proton—averaged over all Fock states as argued in Ref. 3. Dziembowski et al. also show that the perturbative QCD contribution to the form factors dominates over the soft contribution (obtained by convoluting the nonperturbative wave functions) at a scale $Q/N \approx 1$ GeV, where $N$ is the number of valence constituents (see Fig. 13). (This type of criterion was also derived in Ref. 39.) The analysis of Jacob and Kisslinger[40] gives similar estimates for the soft contribution to the pion form factor, as shown in Fig. 14. Earlier claims[41] that a simple overlap of soft hadron wave functions could fit the form factor data were erroneous since they were based on wave functions which violate rotational symmetry in the center-of-mass.

A detailed phenomenological analysis of the nucleon form factors for different shapes of the distribution amplitudes has been given by Ji, Sill
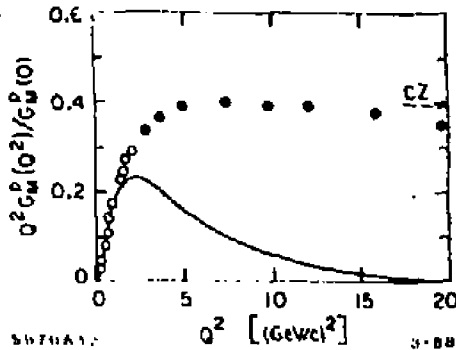
Fig. 13. Comparison of perturbative QCD predictions and data for the proton form factor. The calculation, based on the CZ QCD sum rule distribution amplitude, is from Ref. 42. The prediction depends on the use of the running coupling constant as a function of the exchanged gluon momentum. The data are from Ref. 43.

and Lombard-Nelsen.[42] Their results show that the CZ wave function is consistent with the sign and magnitude of the proton form factor at large $Q^2$ as recently measured by the American University/SLAC collaboration[43] (see Fig. 15).

The normalization of the proton form factor at large $Q^2$ is a nontrivial test of the distribution amplitude shape, for example, if the proton wave function has a nonrelativistic shape peaked at $x_i \sim 1/3$ then one obtains the wrong sign for the nucleon form factor. Furthermore, symmetrical distribution amplitudes predict a very small magnitude for $Q^4 G_M^p(Q^2)$ at large $Q^2$. Gari and Stefanis[44] have developed a model for the nucleon form factors which incorporates the CZ distribution amplitude predictions at high $Q^2$ together with VMD constraints at low $Q^2$. Their analysis predicts sizeable values for the neutron electric form factor at intermediate values of $Q^2$.

Farrar[45] has recently emphasized that the normalization of the nucleon form factor predictions depends strongly on the parameterization of the distribution amplitude at the endpoints. Chernyak et al.[6] have studied this effect in some detail and claim that their QCD sum rule predictions are not significantly changed when higher moments of the distribution amplitude are included. Their results for the neutron form factor, however, disagree with the Gari-Stefanis parameterization.
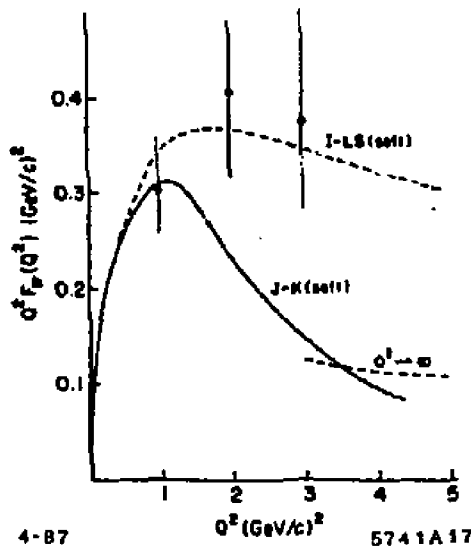
Fig. 14. Model for the "soft" contribution to the pion form factor. The Isgur-Llewellyn-Smith prediction (Ref. 41) is based on a wave function with Gaussian falloff in transverse momentum but power-law falloff at the endpoints in $x$. The Jacob-Kisslinger prediction (Ref. 40) is based on a rotationally symmetric form in the center-of-mass frame. The perturbative QCD contribution calculated with CZ (Ref. 36) distribution amplitudes is consistent with the normalization and shape of the data for $Q^2 > 1$ GeV$^2$.

Measurements of the two-photon exclusive processes $\gamma\gamma \rightarrow \pi^+\pi^-$ and $K^+K^-$ are in excellent agreement with the perturbative QCD predictions. The factorization of the amplitude is illustrated in Fig. 16. The predictions are based on analyses valid to all orders in perturbation theory and do not suffer from the complications of endpoint singularities or pinch contributions. The data[45] (see Fig. 17) extend out to invariant mass squared 10 GeV$^2$, a region well beyond any significant contribution from soft contributions.

Nevertheless, the self-consistency of the perturbative QCD analysis for some exclusive channels can be questioned,[41] particularly for baryon reactions at moderate momentum transfer:

1. The perturbative analysis of the baryon form factor and large angle hadron-hadron scattering depends on the suppression of the endpoint regions $x_i \sim 1$ and pinch singularity contributions. This suppression occurs automatically
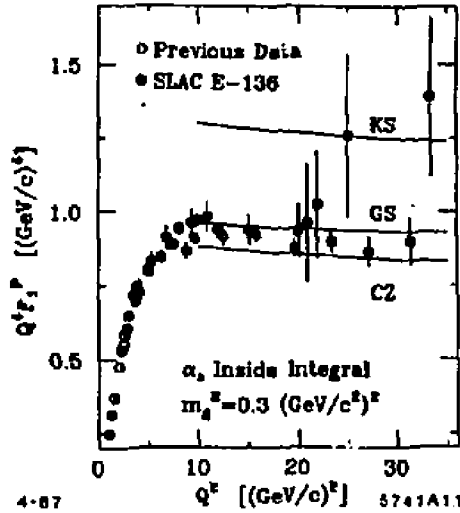
25

Fig. 15. Predictions for the normalization and sign of the proton form factor at high $Q^2$ using perturbative QCD factorization and QCD sum rule predictions for the proton distribution amplitude (Ref. 42). The predictions use forms given by Chernyak and Zhitnitsky, King and Sachrajda (Ref. 37) and Gari and Stefanis (Ref. 44).

in QCD due to Sudakov form factors, as has been shown by Mueller[47] based on the all-orders analysis of the vertex function by Sen.[48] Since these analyses require an all-orders resummation of the vertex corrections, they cannot be derived by standard renormalization group analysis. In this sense the baryon form factor and large angle hadron-hadron scattering results are considered less rigorous than the results from analysis of the meson form factor and the $\gamma\gamma$ production of meson pairs.[49]

2. The magnitude of the proton form factor is sensitive to the $x \sim 1$ dependence of the proton distribution amplitude, where nonperturbative effects could be important. The CZ asymmetric distribution amplitude, in fact, emphasizes contributions from the large $x$ region. Since nonleading corrections are expected when the quark propagator scale $Q^2(1 - x)$ is small, relatively large $Q^2$ is required to clearly test the perturbative QCD predictions. A similar criterion occurs in the analysis of corrections to QCD evolution in deep inelastic lepton scattering. Dziembowski and Mankiewicz[38] find that one can simultaneously fit low energy phenomena (the nucleon magnetic mo-
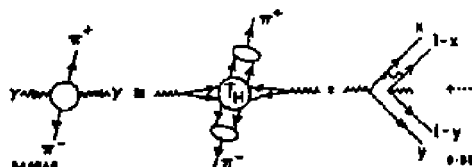
Fig. 16. Application of perturbative QCD factorization to two-photon production of meson pairs.
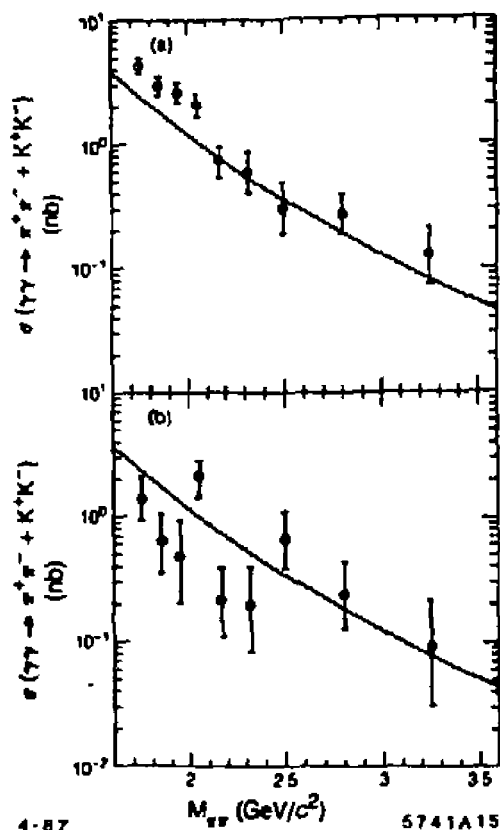


Fig. 17. Measurements from PEP experiments of exclusive two-photon reactions compared with the perturbative QCD predictions of Ref. 49. The predictions are absolutely normalized and nearly independent of the shape of the meson distribution amplitudes since the amplitudes can be related to those appearing in the meson form factor.

ments), the measured high momentum transfer hadron form factors, and the CZ distribution amplitudes with a self-consistent ansatz for the quark wave functions. Thus, for the first time one has a rather complete model for the relativistic 3-quark structure of the nucleon.

## 8. DISCRETIZED LIGHT–CONE QUANTIZATION .

A central goal of QCD analysis is not only to obtain a complete description of the hadronic spectrum but also to evaluate their current matrix elements. Thus, a key problem in the application of QCD to hadron and nuclear physics is how to determine the wave function of a relativistic multiparticle composite system. This is obviously a formidable task. Although composite systems in QCD can be represented formally in terms of the covariant Bethe–Salpeter formalism, calculations beyond ladder approximation appear intractable, and the ladder approximation itself is usually inadequate. For example, in order to derive the Dirac equation for the electron in a static Coulomb field from the Bethe–Salpeter equation for muonium with $m_\mu/m_e \to \infty$, one requires an infinite number of irreducible crossed-graph kernel contributions to the QED potential. Similarily, the matrix elements of currents and the wave function normalization also require, at least formally, the consideration of an infinite sum of irreducible kernels. The relative-time dependence of the Bethe–Salpeter amplitudes for states with three or more constituent fields adds even more complexities.

A more intuitive procedure would be to extend the Schrödinger wave function description of bound states to the relativistic domain by developing a relativistic many-body Fock expansion for the hadronic state. Formally this can be done by quantizing QCD at equal time, and calculating matrix elements from the time-ordered expansion of the $S$-matrix. However, the calculation of each covariant Feynman diagram with $n$-vertices requires the calculation of $n!$ frame-dependent time-ordered amplitudes. Even worse, the calculation of the normalization of a bound state wave function (or the matrix element of a charge or current operator) requires the computation of contributions from all amplitudes involving particle production from the vacuum. (Note that even after normal-ordering, the interaction Hamiltonian density for QED, $H_I = \ : \bar{\psi}\gamma_\mu\psi A^\mu :$, contains contributions $b^\dagger d^\dagger a^\dagger$ which create particles from the perturbative vacuum.) For this reason, it is not possible to represent a relativistic field-theoretic bound system limited to a fixed number of constituents at a given time in a standard Hamiltonian framework

since the interactions create new quanta from the vacuum.[50] Lorentz invariance is also difficult to incorporate in an equal time formalism.

Fortunately, there is a natural and consistent covariant framework, originally due to Dirac,[51] (quantization on the "light front") for describing bound states in gauge theory analogous to the Fock state in nonrelativistic physics. This framework is the light-cone quantization formalism in which

$$|\pi\rangle = |q\bar{q}\rangle\,\psi^\pi_{q\bar{q}} + |q\bar{q}g\rangle\,\psi^\pi_{q\bar{q}g} + \cdots$$

$$|p\rangle = |qqq\rangle\,\psi^p_{qqq} + |qqqg\rangle\,\psi^p_{qqqg} + \cdots .$$

Each wave function component $\psi_n$ describes a state of fixed number of quark and gluon quanta evaluated in the interaction picture at equal light-cone "time" $\tau = t + z/c$. As discussed in the Introduction, given the $\{\psi_n\}$, virtually any hadronic property can be computed, including anomalous moments, form factors, structure functions for inclusive processes, distribution amplitudes for exclusive processes, etc. As shown by Drell and Yan, spacelike form factors are given by a simple overlap of the light-cone wave functions, summed over Fock states.[52] At high momentum transfer only the valence Fock-state enters, to leading order in $1/Q$.

As noted above, in an equal time formalism one must allow for fluctuations in which three or four particles appear with zero total three-momentum. In the light-cone formalism such fluctuations cannot appear since the total $k^+$ is conserved and each particle has to have positive $k^+$. Accordingly, the perturbative vacuum is an eigenstate of the total Hamiltonian on the light-cone. Light-cone quantization and equal $\tau$ wave functions, rather than equal $t$ wave functions, thus provide a sensible Fock state expansion. It also turns out to be convenient to use $\tau$-ordered light-cone perturbation theory in place of covariant perturbation theory to analyze light-cone dominated processes such as deep inelastic scattering and large momentum transfer exclusive reactions. Light-cone quantization and perturbation theory are developed in detail in Ref. 3.

Pauli and I[7] have proposed a direct approach to solving QCD by attempting to diagonalize the light-cone Hamiltonian on a free particle discretized momentum Fock state basis. Since $H_{LC}$, $P^+$, $\vec{P}_\perp$, and the conserved charges all commute, $H_{LC}$ is block diagonal. By choosing periodic (or antiperiodic) boundary conditions for the basis states along the negative light-cone

$$\psi(z^- = +L) = \pm\psi(z^- = -L) ,$$

the Fock basis becomes restricted to finite dimensional representations. The eigen-value problem thus reduces to the diagonalization of a finite Hermitian matrix. To see this, note that periodicity in $z^-$ requires

$$P^+ = \frac{2\pi}{L}K \ , \qquad k_i^+ = \frac{2\pi}{L}\, n_i \ , \qquad \sum_{i=1}^{n} n_i = K \ .$$

The dimension of the representation corresponds to the number of partitions of the integer $K$ as a sum of positive integers $n$. For a finite resolution $K$, the wave function is sampled at the discrete points

$$x_i = \frac{k_i^+}{P^+} = \frac{n_i}{K} = \left\{ \frac{1}{K}, \frac{2}{K}, \cdots \frac{K-1}{K} \right\} \ .$$

The continuum limit is clearly $K \to \infty$.

One can easily show that $P^-$ scales as $L$. We thus define $P^- \equiv \frac{L}{2\pi} H$. The eigenstates with $P^2 = M^2$ at fixed $P^+$ and $\vec{P}_\perp = 0$ thus satisfy

$$H_{LC}\, |\Psi\rangle = KH\, |\Psi\rangle = M^2\, |\Psi\rangle \ ,$$

independent of $L$ (which corresponds to a Lorentz boost factor).

The basis of the DLCQ method is thus conceptually simple: one quantizes the independent fields at equal light-cone time $\tau$ and requires them to be periodic or antiperiodic in light-cone space with period $2L$. The commuting operators, the light-cone momentum $P^+ = \frac{2\pi}{L}K$ and the light-cone energy $P^- = \frac{L}{2\pi}H$ are constructed explicitly in a Fock space representation and diagonalized simultane-ously. The eigenvalues give the physical spectrum: the invariant mass squared $M^2 = P^\nu P_\nu$. The eigenfunctions give the wave functions at equal $\tau$ and allow one to compute the current matrix elements, structure functions and distribution amplitudes required for physical processes. All of these quantities are manifestly independent of $L$, since $M^2 = P^+ P^- = HK$. Lorentz-invariance is violated by periodicity, but reestablished at the end of the calculation by going to the contin-uum limit: $L \to \infty$, $K \to \infty$ with $P^+$ finite. In the case of gauge theory, the use of the light-cone gauge $A^+ = 0$ eliminates negative metric states in both Abelian and non–Abelian theories.

Since continuum as well as single hadron color singlet hadronic wave func-tions are obtained by the diagonalization of $H_{LC}$, one can also calculate scattering amplitudes as well as decay rates from overlap matrix elements of the interaction Hamiltonian for the weak or electromagnetic interactions. An important point is that all higher Fock amplitudes including spectator gluons are kept in the light-

cone quantization approach; such contributions cannot generally be neglected in decay amplitudes involving light quarks.

Eller, Pauli and I[53] have used DLCQ to obtain detailed results for the bound state and continuum spectrum and wave functions for QED in one-space and one-time dimension for arbitrary mass and coupling constant. I will give here only a brief discussion of the method. The commuting operators $K$, $Q$ and $H = H_0 + V$ have the form

$$K = \sum n(b_n^\dagger b_n + d_n^\dagger d_n) + n(a_n^\dagger a_n)$$

$$Q = \sum (b_n^\dagger b_n - d_n^\dagger d_n)$$

$$H_0 = \sum \frac{m_\perp^2}{n} (b_n^\dagger b_n + d_n^\dagger d_n) + \frac{k_\perp^2}{n} a_n^\dagger a_n$$

$$V = \frac{g^2}{\pi} \sum_{n \neq m, k \neq \ell} b_k^\dagger b_\ell d_n^\dagger d_m \frac{\delta_{n+k, m+\ell}}{(n-m)^2} + \cdots .$$

Only the one fermion antifermion (Abelian) interaction, corresponding to "instantaneous" gluon exchange, is displayed. The $Q = 0$ Fock state basis states are of the form

$$b_n^\dagger d_m^\dagger a_\ell^\dagger |0\rangle = |n; m; \ell\rangle$$

$(n + m + \ell = K)$ where $|0\rangle$ is the perturbative vacuum. (Spin, color and transverse momentum for any number of dimensions are represented as extra internal variables.) We then solve

$$HK |\Psi\rangle = M^2 |\Psi\rangle$$

on the free particle basis

$$|\Psi\rangle = \sum_i C_i |i\rangle .$$

Note that the eigenvalues of $H_{LC}$ give not only the bound state spectrum, but also all of the multiparticle scattering states with the same quantum numbers.

In the case of gauge theory in 3+1 dimensions, one also takes the $k_\perp^i = (2\pi/L_\perp)n_\perp^i$ as discrete variables on a finite cartesian basis. The theory is covariantly regulated if one restricts states by the condition

$$\sum_i \frac{k_{\perp i}^2 + m_i^2}{z_i} \leq \Lambda^2 ,$$

where $\Lambda$ is the ultraviolet cutoff. In effect, states with total light-cone kinetic energy beyond $\Lambda^2$ are cut off. In a renormalizable theory physical quantities are independent of physics beyond the ultraviolet regulator; the only dependence on $\Lambda$ appears in the coupling constant and mass parameters of the Hamiltonian, consistent with the renormalization group.[54] The resolution parameters need to be taken sufficiently large such that the theory is controlled by the continuum regulator $\Lambda$, rather than the discrete scales of the momentum space basis.

The simplest application of DLCQ to local gauge theory is QED in one-space and one-time dimensions. Since $A^+ = 0$ is a physical gauge there are no photon degrees of freedom. Explicit forms for the matrix representation of $H_{QED}$ are given in Ref. 53. The basic interactions which occur in $H_{LC}$ (QCD) are illustrated in Fig. 18.
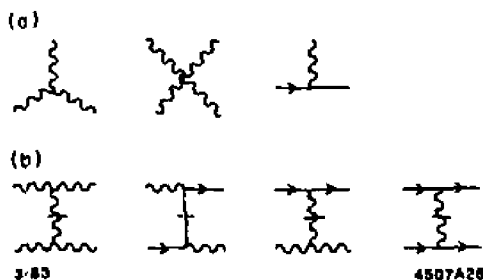


Fig. 18. Diagrams which appear in the interaction Hamiltonian for QCD on the light-cone. The propagators with horizontal bars represent instantaneous gluon and quark exchange which arise from reduction of the dependent fields in $A^+ = 0$ gauge.

For the general case $m^2 \neq 0$, $(QED)_{1+1}$ can be solved by numerical diagonalization. The complete charge zero spectrum (normalized to the ground state mass) for $K = 16$ is shown as a function of coupling constant in Fig. 19. Since the physics can only depend on the ratio $m/g$, it is convenient to introduce the parametrization

$$\lambda = \sqrt{\frac{1}{1 + \pi(m/g)^2}}$$

which maps the entire range of $m$ and $g$ onto the finite interval $0 \leq \lambda \leq 1$.

In the zero coupling limit the spectrum is that of the free theory. In the infinite coupling limit $\lambda = 1$ the theory is essentially equivalent to the limit of

zero fermion mass. Schwinger has shown that massless $(QED)_{1+1}$ is equivalent to a free boson theory. In the light-cone formalism one can solve the $m = 0$ theory explicitly. One defines[55] bilinear operators in the fermion fields $a_n$ and $a_n^\dagger$ which have normal boson commutation rules. Then for $Q = 0$

$$H = m^2 \sum_{n+1}^{\infty} \frac{1}{n} \left( b_n^\dagger b_n + d_n^\dagger d_n \right) + \frac{g^2}{\pi} \sum_{n=1}^{\infty} \frac{1}{n} \, a_n^\dagger a_n \; .$$

Thus, for $m^2 = 0$ (or $g^2/\pi \gg m^2$), $H_{\text{QED}}$ is equivalent to free boson theory with $m_g^2 = g^2/\pi$. The distinction between the theories in the limit of zero fermion mass is discussed by McCartor.[56]
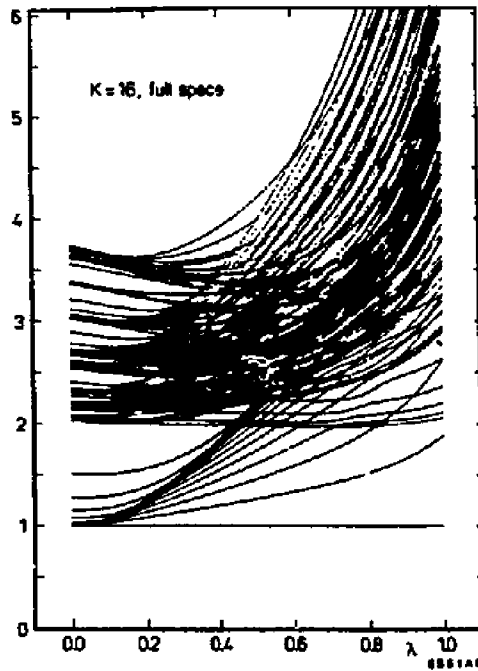


Fig. 19. Spectrum of QED in one-space and one-time dimension for harmonic resolution $K = 16$. The ratios $M_i/M_1$ are plotted as a function of the scaled coupling constant $\lambda$. The Schwinger limit is $\lambda = 1$ (Ref. 53).

Figure 20 shows the structure function for the ground state of $(QED)_{1+1}$ as a function of $\lambda$. In the weak binding limit $g \to 0$ or ($m \to \infty$), the structure function becomes a delta function at equal partition of the constituent momentum,

33

as expected. In the strong coupling limit $g \rightarrow \infty$ $(m \rightarrow 0)$ the structure function becomes flat. This is consistent with the interpretation of the Schwinger boson as a point-like composite of a fermion and antifermion. The contribution to higher Fock states to the lowest mass structure function is strikingly small; the probability of nonvalence states is less than 1% for any value of $\lambda$.
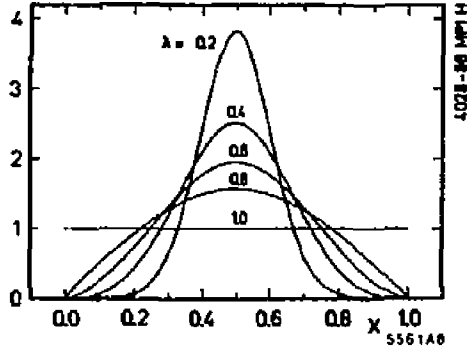


Fig. 20. The structure function of the lowest mass bound state for QED in 1+1 space-time dimensions, as calculated in the DLCQ formalism (Ref. 53).

It is interesting that there is analytic agreement between the DLCQ results and the exact solutions of the Schwinger model for finite $K$, as well as in the continuum limit. This can be traced to the fact that the structure function of the Schwinger boson is flat and thus needs minimal resolution. In the case of the massive Schwinger model $(QED_2)$, we established the existence of the continuum limit numerically; for sufficiently large resolution $K$ the results become independent of $K$. The essential criteria for convergence is that the intrinsic dynamical structure of the wave functions is sufficiently resolved at the rational values $x = n/K$, $n = 1, 2, ..., K - 1$ accessible at a given $K$.

In the large $K$ limit, the eigenvalues agree quantitatively with the results of Bergknoff[55] and with those of a lattice gauge calculation by Crewther and Hamer.[57] This result is important in establishing the equivalence of different complementary nonperturbative methods. We also verified numerically that different Fock space representations yield the same physical results. In particular, we solved the $QED_2$ spectrum in the space corresponding to the solutions of the free, massive Dirac equation $(i\gamma^\mu \partial_\mu + m_F)\psi = 0$ as well as of the massless equation $i\gamma^\mu \partial_\mu \psi = 0$. Convergence is slow in $1/K$ only at very large coupling $\lambda$ near one.

Even for moderately large values of the resolution, DLCQ provides one with a qualitatively correct picture of the whole spectrum of eigenfunctions. This aspect becomes important for the development of scattering theory within the DLCQ approach. For example, we have found the rather surprising result that the lowest eigenfunction has very small probability (less than 1%) for $|2f;2\bar{f}\rangle$ and higher particle Fock states (i.e., no 'sea quarks'). We have also obtained the spectrum of the Yukawa theory with spin-zero bosons, a theory with a more complicated Fock structure. Also, Harindranath and Vary[58] have recently used a DLCQ approach to analyze $\phi^4$ theory, a model with a nontrivial vacuum structure.

Recently, Hornbostel[59] has used DLCQ to obtain the complete color-singlet spectrum of QCD in one-space and one-time dimension for $N_C = 2,3,4$. The hadronic spectra are obtained as a function of quark mass and QCD coupling constant (see Fig. 21). Where they are available, the spectra agree with results obtained earlier; in particular, the lowest meson mass in SU(2) agrees within errors with lattice Hamiltonian results.[60] The meson mass at $N_C = 4$ is close to the value obtained in the large $N_C$ limit. The method also provides the first results for the baryon spectrum in a non–Abelian gauge theory. The lowest baryon mass is shown in Fig. 21(b) as a function of coupling constant. The ratio of meson to baryon mass as a function of $N_C$ also agrees at strong coupling with results obtained by Frishman and Sonnenschein.[61] Precise values for the mass eigenvalue can be obtained by extrapolation to large $K$ since the functional dependence in $1/K$ is understood.

As emphasized above, when the light-cone Hamiltonian is diagonalized for a finite resolution $K$, one gets a complete set of eigenvalues corresponding to the total dimension of the Fock state basis. A representative example of the spectrum is shown in Fig. 22 for baryon states $(B = 1)$ as a function of the dimensionless variable $\lambda = 1/\sqrt{1 + \pi m^2/g^2}$. Antiperiodic boundary conditions are used. Note that spectrum automatically includes continuum states with $B = 1$.

The structure functions for the lowest meson and baryon states in SU(3) at two different coupling strengths $m/g = 1.6$ and $m/g = 0.1$ are shown in Figs. 23 and 24. Higher Fock states have a very small probability; representative contributions to the baryon structure functions are shown in Figs. 25 and 26. For comparison, the valence wave function of a higher mass state which can be identified as a composite of meson pairs (analogous to a nucleus) is shown in Fig. 27.
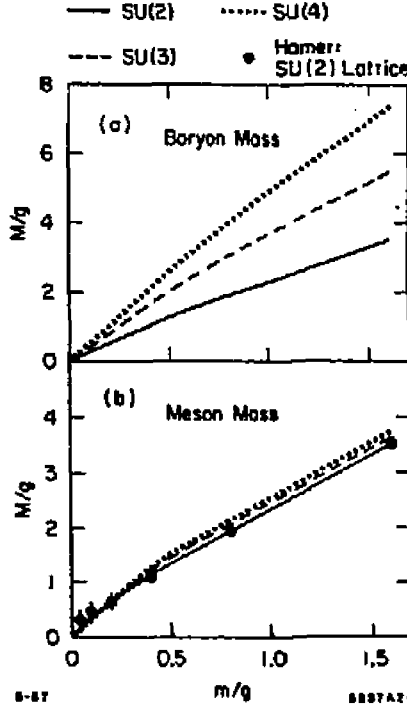
Fig. 21. The baryon and meson spectrum in QCD [1+1] computed in DLCQ for $N_C = 2, 3, 4$ as a function of quark mass and coupling constant (Ref. 59).

The interactions of the quarks in the pair state produce Fermi motion beyond $x = 0.5$.

There are a number of important advantages of the DLCQ method which have emerged from this study of two-dimensional field theories.

1. The Fock space is denumerable and finite in particle number for any fixed resolution $K$. In the case of gauge theory in 3+1 dimensions, one expects that photon or gluon quanta with zero four-momentum decouple from neutral or color-singlet bound states, and thus need not be included in the Fock basis. The transverse momenta are additive and can be introduced on a Cartesian grid. Hornbostel[59] has developed methods to implement the color degrees of freedom for the non–Abelian theories. Tang[62] is currently studying QED[3+1] in DLCQ as a function of the QED coupling constant.
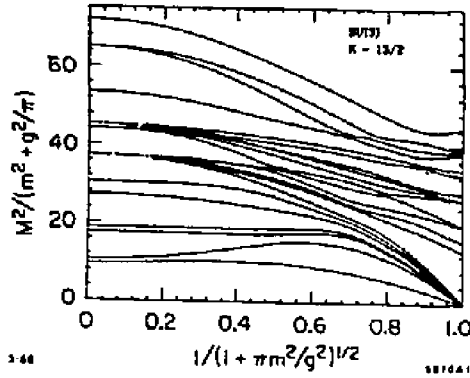
**Fig. 22.** Representative baryon spectrum for QCD in one-space and one-time dimension (Ref. 59).
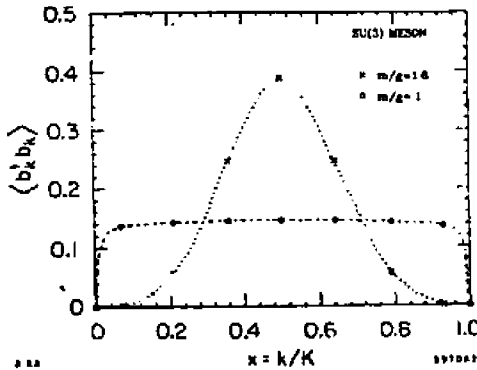


**Fig. 23.** The meson quark momentum distribution in QCD [1+1] computed using DLCQ (Ref. 59).

2. Because we are using discrete momentum-space representation, rather than a space-time lattice, there are no special difficulties with fermions, e.g., no fermion doubling, fermion determinants or necessity for a quenched approximation. Furthermore, the discretized theory has basically the same ultra-violet structure as the continuum theory. It should be emphasized that, unlike lattice calculations, there is no constraint or relationship between the physical size of the bound state and the length scale $L$.
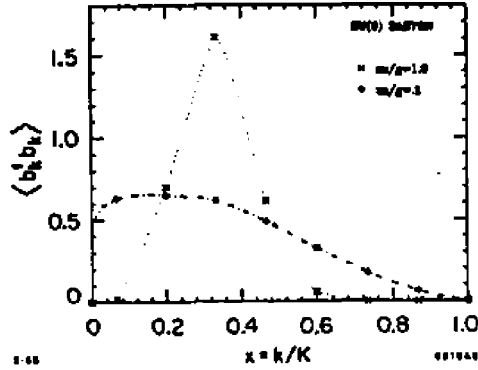
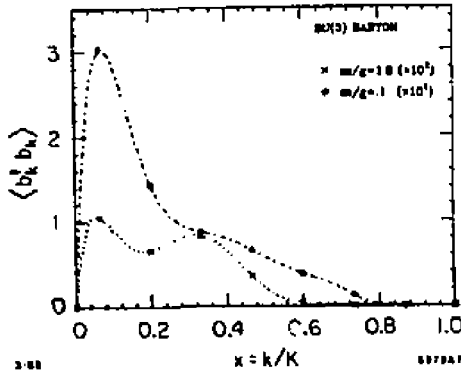Fig. 24. The baryon quark momentum distribution in QCD [1+1] computed using DLCQ (Ref. 59).



Fig. 25. Contibution to the baryon quark momentum distribution from $qqqq\bar{q}$ states for QCD[1+1] (Ref. 59).

3. The DLCQ method has the remarkable feature of generating the complete spectrum of the theory; bound states and continuum states alike. These can be separated by tracing their minimum Fock state content down to small coupling constant since the continuum states have higher particle number content. In lattice gauge theory it appears intractable to obtain information on excited or scattering states or their correlations. The wave functions
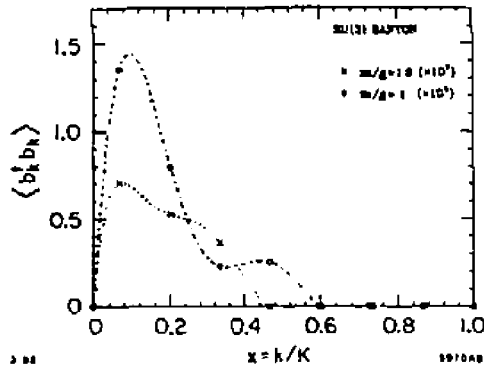
Fig. 26. Contibution to the baryon quark momentum distribution from $qqqq\bar{q}\bar{q}$ states for QCD[1+1] (Ref. 59).
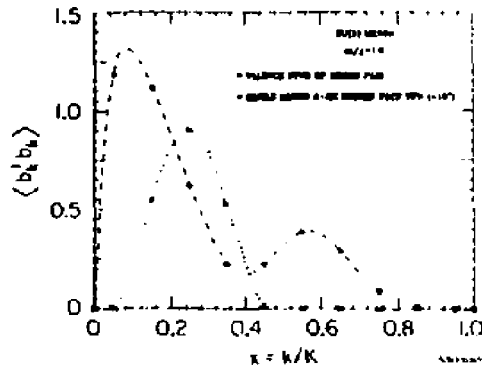


Fig. 27. Comparison of the meson quark distributions in the $qq\bar{q}\bar{q}$ Fock state with that of a continuum meson pair state. The structure in the former may be due to the fact that these four-particle wave functions are orthogonal. The analysis is for $N_C = 2$ in 1+1 dimensions (Ref. 59).

generated at equal light-cone time have the immediate form required for relativistic scattering problems.

4. DLCQ is basically a relativistic many-body theory, including particle number creation and destruction, and is thus a basis for relativistic nuclear and atomic problems. In the nonrelativistic limit the theory is equivalent to many-body Schrödinger theory.

The immediate goal is gauge theory in 3+1 dimensions. Already Klabucar and Pauli[63] have studied QCD[3+1] in the $q\bar{q}$ sector for strong coupling. In the Abelian case it will be interesting to analyze QED and the positronium spectrum in the large $\alpha$ limit. Whether the non–Abelian theory can be solved using DLCQ—considering its greater number of degrees of freedom and its complex equal-time vacuum—is an open question. The studies for Abelian and non–Abelian gauge theory carried out so far in 1+1 dimensions give grounds for optimism.

9. SPIN CORRELATIONS, QCD COLOR TRANSPARENCY
   AND HEAVY QUARK THRESHOLDS IN $pp$ SCATTERING

One of the most serious challenges to quantum chromodynamics is the behavior of the spin-spin correlation asymmetry $A_{NN} = \frac{[d\sigma(\uparrow\uparrow)-d\sigma(\uparrow\downarrow)]}{[d\sigma(\uparrow\uparrow)+d\sigma(\uparrow\downarrow)]}$ measured in large momentum transfer $pp$ elastic scattering (see Fig. 4). At $p_{lab} = 11.75$ GeV/c and $\theta_{cm} = \pi/2$, $A_{NN}$ rises to $\simeq 60\%$, corresponding to four times more probability for protons to scatter with their incident spins both normal to the scattering plane and parallel, rather than normal and opposite. The polarized cross section shows a striking energy and angular dependence not expected from the slowly-changing perturbative QCD predictions.[64] However, the unpolarized data is in first approximation consistent with the fixed angle scaling law $s^{10}d\sigma/dt(pp \rightarrow pp) = f(\theta_{CM})$ expected from the perturbative analysis (see Fig. 28).

The onset of new structure[65] at $s \simeq 23$ GeV$^2$ is a sign of new degrees of freedom in the two-baryon system. In this section I discuss an explanation by Guy de Teramond and myself[18] for (1) the observed spin correlations, (2) the deviations from fixed-angle scaling laws and (3) the anomalous energy dependence of absorptive corrections to quasi-elastic $pp$ scattering in nuclear targets, in terms of a simple model based on two $J = L = S = 1$ broad resonances (or threshold enhancements) interfering with a perturbative QCD quark-interchange background amplitude. The structures in the $pp \rightarrow pp$ amplitude may be associated with the onset of strange and charmed thresholds. If this view is correct, large angle $pp$ elastic scattering would have been virtually featureless for $p_{lab} \geq 5$ GeV/c, had it not been for the onset of heavy flavor production. As a further illustration of the threshold effect, we also show the effect in $A_{NN}$ due to a narrow $^3F_3$ $pp$ resonance at $\sqrt{s} = 2.17$ GeV ($p_{lab} = 1.26$ GeV/c) associated with the $p\Delta$ threshold.

The perturbative QCD analysis[66] of exclusive amplitudes assumes that large momentum transfer exclusive scattering reactions are controlled by short
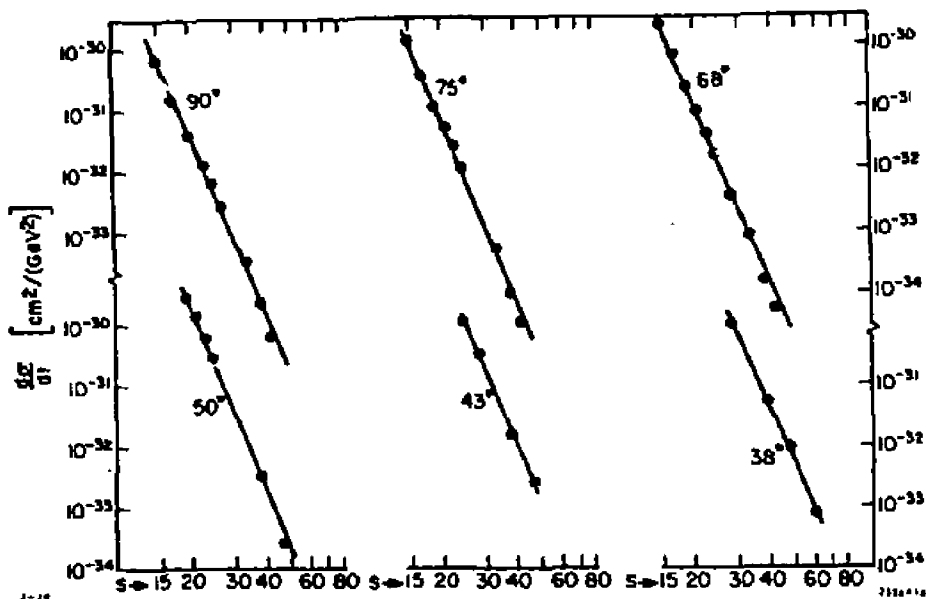
Fig. 28. Test of fixed $\theta_{CM}$ scaling for elastic $pp$ scattering. The best fit gives the power $N = 9.7 \pm 0.5$ compared to the dimensional counting prediction N=10. Small deviations are not readily apparent on this log-log plot. The compilation is from Landshoff and Polkinghorne.

distance quark-gluon subprocesses, and that corrections from quark masses and intrinsic transverse momenta can be ignored. The main predictions are fixed-angle scaling laws[67] (with small corrections due to evolution of the distribution amplitudes, the running coupling constant and pinch singularities), hadron-helicity conservation[68] and the novel phenomenon discussed in the Introduction called "color transparency."

As discussed in Sec. 7. the power-law scaling quark-counting predictions for form factors, two-body elastic hadron-hadron scattering,[69] and exclusive two-photon reactions are generally consistent with experiment at transverse momenta beyond a few GeV. (See Figs. 14, 15, 17 and 28.) In leading order in $1/p_T$, only the lowest particle-number "valence" Fock state wave function with all the quarks within an impact distance $b_\perp \leq 1/p_T$ contributes to the high momentum transfer scattering amplitude in QCD. Such a Fock state component has a small color dipole moment and thus interacts only weakly with hadronic or nuclear matter.[16] This minimally interacting proton configuration can retain its small size

as it propagates in the nucleus over a distance which grows with energy. Thus, unlike traditional Glauber theory, QCD predicts that large momentum transfer quasi-elastic reactions occurring in a nucleus suffer minimal initial and final state attenuation, i.e., one expects a volume rather than surface dependence in the nuclear number. This is the QCD "color transparency" prediction.

As discussed in the Introduction, a test of color transparency in large momentum transfer quasi-elastic $pp$ scattering at $\theta_{cm} \simeq \pi/2$ has recently been carried out at BNL using several nuclear targets (C, Al, Pb).[17] The attenuation at $p_{lab} = 10$ GeV/c in the various nuclear targets was observed to be in fact much less than that predicted by traditional Glauber theory (see Fig. 1). This appears to support the color transparency prediction. However, at $p_{lab} = 12$ GeV/c, normal attenuation was observed, in contradiction to the expectation from perturbative QCD that the transparency effect should become even more apparent! Our observation is that one can explain this surprising result if the scattering at $p_{lab} = 12$ GeV/c ($\sqrt{s} = 4.93$ GeV), is dominated by an $s$-channel B=2 resonance (or resonance-like structure) with mass near 5 GeV, since unlike a hard scattering reaction, a resonance couples to the fully-interacting large-scale structure of the proton. If the resonance has spin $S = 1$, this can also explain the large spin correlation $A_{NN}$ measured nearly at the same momentum, $p_{lab} = 11.75$ GeV/c. Conversely, in the momentum range $p_{lab} = 5$ to 10 GeV/c we predict that the perturbative hard-scattering amplitude is dominant at large angles. The experimental observation of diminished attenuation at $p_{lab} = 10$ GeV/c thus provides support for the QCD description of exclusive reactions and color transparency.

What could cause a resonance at $\sqrt{s} = 5$ GeV, more than 3 GeV beyond the $pp$ threshold? We can think of several possibilities: (a) a multigluonic excitation such as $|qqqqqqqggg\rangle$, (b) a "hidden color" color singlet $|qqqqqq\rangle$ excitation[70] or (c) a "hidden flavor" $|qqqqqqQ\overline{Q}\rangle$ excitation, which is the most interesting possibility, since it is so predictive. As in QED, where final state interactions give large enhancement factors for attractive channels in which $Z\alpha/v_{rel}$ is large, one expects resonances or threshold enhancements in QCD in color-singlet channels at heavy quark production thresholds since all the produced quarks have similar velocities.[71] One thus can expect resonant behavior at $M^* = 2.55$ GeV and $M^* = 5.08$ GeV, corresponding to the threshold values for open strangeness: $pp \rightarrow \Lambda K^+ p$, and open charm: $pp \rightarrow \Lambda_c D^0 p$, respectively. In any case, the

structure at 5 GeV is highly inelastic: we find that its branching ratio to the proton-proton channel is $B^{pp} \simeq 1.5\%$.

We now proceed to a description of the model. We have purposely attempted not to overcomplicate the phenomenology; in particular, we have used the simplest Breit–Wigner parameterization of the resonances, and we have not attempted to optimize the parameters of the model to obtain a best fit. It is possible that what we identify as a single resonance is actually a cluster of resonances.

The background component of the model is the perturbative QCD amplitude. Although complete calculations are not yet available, many features of the QCD predictions are understood, including the approximate $s^{-4}$ scaling of the $pp \rightarrow pp$ amplitude at fixed $\theta_{cm}$ and the dominance of those amplitudes that conserve hadron helicity.[68] Furthermore, recent data comparing different exclusive two-body scattering channels from BNL[69] show that quark interchange amplitudes[72] dominate quark annihilation or gluon exchange contributions. Assuming the usual symmetries, there are five independent $pp$ helicity amplitudes: $\phi_1 = M(++,++)$, $\phi_2 = M(--,++)$, $\phi_3 = M(+-,+-)$, $\phi_4 = M(-+,+-)$, $\phi_5 = M(++,+-)$. The helicity amplitudes for quark interchange have a definite relationship.[64] For definiteness, we will assume the following form

$$\phi_1(\text{PQCD}) = 2\phi_3(\text{PQCD}) = -2\phi_4(\text{PQCD})$$

$$= 4\pi C\, F(t) F(u) [\frac{t - m_d^2}{u - m_d^2} + (u \leftrightarrow t)] e^{i\delta} .$$

The hadron helicity nonconserving amplitudes, $\phi_2(\text{PQCD})$ and $\phi_5(\text{PQCD})$ are zero. This form is consistent with the nominal power-law dependence predicted by perturbative QCD[66] and also gives a good representation of the angular distribution over a broad range of energies.[73] Here $F(t)$ is the helicity-conserving proton form factor, which for simplicity, we take as the standard dipole form, $F(t) = (1 - t/m_d^2)^{-2}$, with $m_d^2 = 0.71$ GeV$^2$. As shown in Ref. 64, the PQCD quark-interchange structure alone predicts $A_{NN} \simeq 1/3$, nearly independent of energy and angle.

Because of the rapid fixed-angle $s^{-4}$ falloff of the perturbative QCD amplitude, even a very weakly-coupled resonance can have a sizeable effect at large momentum transfer. The large empirical values for $A_{NN}$ suggest a resonant $pp \rightarrow pp$ amplitude with $J = L = S = 1$ since this gives $A_{NN} = 1$ (in absence of background) and a smooth angular distribution. Because of the Pauli

principle, an $S = 1$ di-proton resonance must have odd parity and thus odd orbital angular momentum. We parameterize the two non-zero helicity amplitudes for a $J = L = S = 1$ resonance in Breit–Wigner form:

$$\phi_3(\text{resonance}) = 12\pi \frac{\sqrt{s}}{p_{cm}} d^1_{1,1}(\theta_{cm}) \frac{\frac{1}{2}\Gamma^{pp}(s)}{M^* - E_{cm} - \frac{1}{2}\Gamma} \,,$$

$$\phi_4(\text{resonance}) = -12\pi \frac{\sqrt{s}}{p_{cm}} d^1_{-1,1}(\theta_{cm}) \frac{\frac{1}{2}\Gamma^{pp}(s)}{M^* - E_{cm} - \frac{1}{2}\Gamma} \,.$$

(The $^3F_3$ resonance amplitudes have the same form with $d^3_{\pm1,1}$ replacing $d^1_{\pm1,1}$.) Since we are far from threshold, threshold factors in the $pp$ channel can be treated as constants. As in the case of a narrow resonance like the $Z^0$, we expect that the partial width into nucleon pairs is proportional to the square of the time-like proton form factor: $\Gamma^{pp}(s)/\Gamma = B^{pp}|F(s)|^2/|F(M^{*2})|^2$, corresponding to the formation of two protons at this invariant energy. The resonant amplitudes then die away by one inverse power of $(E_{cm} - M^*)$ relative to the dominant PQCD amplitudes. (In this sense, they are higher twist contributions relative to the leading twist perturbative QCD amplitudes.) The model is thus very simple: each $pp$ helicity amplitude $\phi_i$ is the coherent sum of PQCD plus resonance components: $\phi = \phi(\text{PQCD}) + \Sigma\phi(\text{resonance})$. Because of pinch singularities and higher order corrections, the hard QCD amplitudes are expected to have a nontrivial phase;[74] we have thus allowed for a constant phase $\delta$ in $\phi(\text{PQCD})$. Because of the absence of the $\phi_5$ helicity-flip amplitude, the model predicts zero single spin asymmetry $A_N$. This is consistent with the large angle data at $p_{lab} = 11.75$ GeV/c.[75]

At low transverse momentum, $p_T \leq 1.5$ GeV, the power-law falloff of $\phi(\text{PQCD})$ in $s$ disagrees with the more slowly falling large-angle data, and we have little guidance from basic theory. Our interest in this low energy region is to illustrate the effects of resonances and threshold effects on $A_{NN}$. In order to keep the model tractable, we have simply extended the background quark interchange and the resonance amplitudes at low energies using the same forms as above but replacing the dipole form factor by a phenomenological form $F(t) \propto e^{-\frac{1}{2}\beta\sqrt{|t|}}$. We have also included a kinematic factor of $\sqrt{s}/2p_{cm}$ in the background amplitude. The value $\beta = 0.85$ GeV$^{-1}$ then gives a good fit to $d\sigma/dt$ at $\theta_{cm} = \pi/2$ for $p_{lab} \leq 5.5$ GeV/c.[76] The normalizations are chosen to maintain continuity of the amplitudes.

The predictions of the model and comparison with experiment are shown in Figs. 29 through 34. The following parameters are chosen: $C = 2.9 \times 10^3$, $\delta = -1$ for the normalization and phase of $\phi(\text{PQCD})$. The mass, width and $pp$ branching ratio for the three resonances are $M_d^* = 2.17$ GeV, $\Gamma_d = 0.04$ GeV, $B_d^{pp} = 1$; $M_s^* = 2.55$ GeV, $\Gamma_s = 1.6$ GeV, $B_s^{pp} = 0.65$; and $M_c^* = 5.08$ GeV, $\Gamma_c = 1.0$ GeV, $B_c^{pp} = 0.0155$; respectively. As shown in Figs. 29 and 30, the deviations from the simple scaling predicted by the PQCD amplitudes are readily accounted for by the resonance structures. The cusp which appears in Fig. 30 marks the change in regime below $p_{lab} = 5.5$ GeV/c where PQCD becomes inapplicable. It is interesting to note that in this energy region normal attenuation of quasi-elastic $pp$ scattering is observed.[17] The angular distribution (normalized to the data at $\theta_{cm} = \pi/2$) is predicted to broaden relative to the steeper perturbative QCD form, when the resonance dominates. As shown in Fig. 31 this is consistent with experiment, comparing data at $p_{lab} = 7.1$ and 12.1 GeV/c.
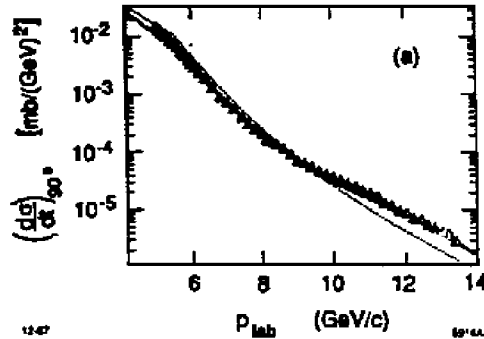


Fig. 29. Prediction (solid curve) for $d\sigma/dt(pp \to pp)$ at $\theta_{cm} = \pi/2$ compared with the data of Akerlof et al. (Ref. 76). The dotted line is the background PQCD prediction.

The most striking test of the model is its prediction for the spin correlation $A_{NN}$ shown in Fig. 32. The rise of $A_{NN}$ to $\simeq 60\%$ at $p_{lab} = 11.75$ GeV/c is correctly reproduced by the high energy J=1 resonance interfering with $\phi(\text{PQCD})$. The narrow peak which appears in the data of Fig. 32 corresponds to the onset of the $pp \to p\Delta(1232)$ channel which can be interpreted as a $uuuudd\bar{q}q$ resonant state. Because of spin-color statistics, in this case one expects a higher orbital momentum state, such as a $pp\,^3F_3$ resonance. The model is also consistent with the recent high energy data point for $A_{NN}$ at $p_{lab} = 18.5$ GeV/c and $p_T^2 = 4.7$ GeV$^2$ (see Fig. 33).
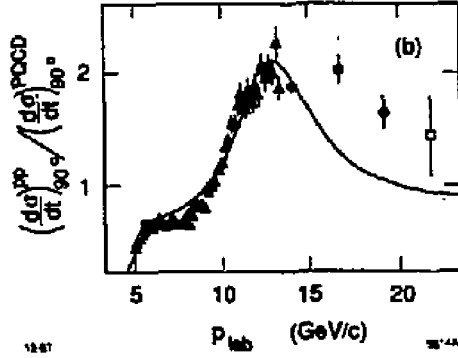
Fig. 30. Ratio of $d\sigma/dt(pp \to pp)$ at $\theta_{cm} = \pi/2$ to the PQCD prediction. The data (Ref. 76) are from Akerlof et al. (open triangles), Allaby et al. (solid dots) and Cocconi et al. (open square). The cusp at $p_{lab} = 5.5$ GeV/c indicates the change of regime from PQCD.
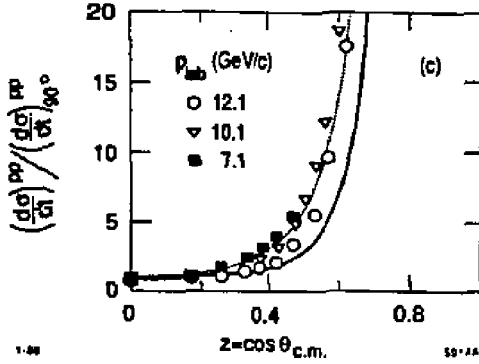


Fig. 31. The $pp \to pp$ angular distribution normalized at $\theta_{cm} = \pi/2$. The data are from the compilation given in Sivers et al. (Ref. 69). The solid and dotted lines are predictions for $p_{lab} = 12.1$ and 7.1 GeV/c, respectively, showing the broadening near resonance.

The data show a dramatic decrease of $A_{NN}$ to zero or negative values. This is explained in our model by the destructive interference effects above the resonance region. The same effect accounts for the depression of $A_{NN}$ for $p_{lab} \approx 6$ GeV/c shown in Fig. 32. The comparison of the angular dependence of $A_{NN}$ with data at $p_{lab} = 11.75$ GeV/c is shown in Fig. 34. The agreement with the data[77] for the longitudinal spin correlation $A_{LL}$ at the same $p_{lab}$ is somewhat worse.
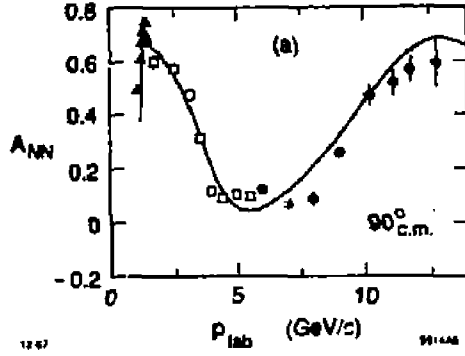
46

Fig. 32. $A_{NN}$ as a function of $p_{lab}$ at $\theta_{cm} = \pi/2$. The data (Ref. 1) are from Crosbie et al. (solid dots), Lin et al. (open squares) and Bhatia et al. (open triangles). The peak at $p_{lab} = 1.26$ GeV/c corresponds to the $p\Delta$ threshold. The data are well reproduced by the interference of the broad resonant structures at the strange ($p_{lab} = 2.35$ GeV/c) and charm ($p_{lab} = 12.8$ GeV/c) thresholds, interfering with a PQCD background. The value of $A_{NN}$ from PQCD alone is 1/3.
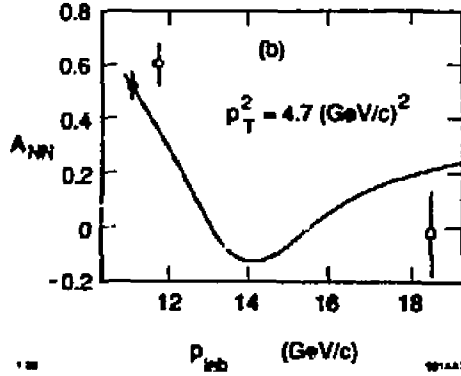


Fig. 33. $A_{NN}$ at fixed $p_T^2 = 4.7$ (GeV/c)$^2$. The data point (Ref. 1) at $p_{lab} = 18.5$ GeV/c is from Court et al.

Thus far we have not attempted a a global fit to all the $pp$ elastic scattering data, but rather to show that many features can be naturally explained with only a few ingredients: a perturbative QCD background plus resonant amplitudes associated with rapid changes of the inelastic $pp$ cross section. The model provides a good description of the $s-$ and $t$-dependence of the differential cross section,
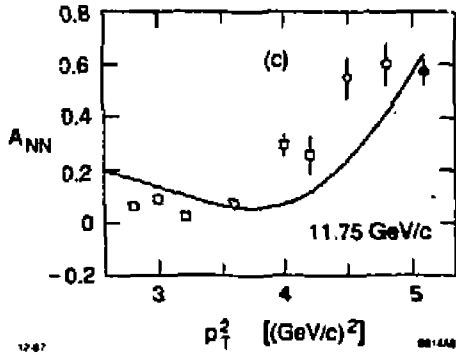
Fig. 34. $A_{NN}$ as a function of transverse momentum. The data (Ref. 1) are from Crabb et al. (open circles) and O'Fallon et al. (open squares). Diffractive contributions should be included for $p_T^2 \leq 3$ GeV$^2$.

including its "oscillatory" dependence[78] in $s$ at fixed $\theta_{cm}$, and the broadening of the angular distribution near the resonances. Most important, it gives a consistent explanation for the striking behavior of both the spin-spin correlations and the anomalous energy dependence of the attenuation of quasi-elastic $pp$ scattering in nuclei. We predict that color transparency should reappear at higher energies ($p_{lab} \geq 16$ GeV/c), and also at smaller angles ($\theta_{cm} \approx 60°$) at $p_{lab} = 12$ GeV/c where the perturbative QCD amplitude dominates. If the J=1 resonance structures in $A_{NN}$ are indeed associated with heavy quark degrees of freedom, then the model predicts inelastic $pp$ cross sections of the order of 1 mb and 1 $\mu b$ for the production of strange and charmed hadrons near their respective thresholds.[79] Thus, a crucial test of the heavy quark hypothesis for explaining $A_{NN}$, rather than hidden color or gluonic excitations, is the observation of significant charm hadron production at $p_{lab} \geq 12$ GeV/c. Other elastic reactions such as $\pi p \rightarrow \pi p$ should also display structures at the corresponding heavy quark thresholds.

## 10.    EXCLUSIVE NUCLEAR PROCESSES IN QCD

One of the most elegant areas of application of QCD to nuclear physics is the domain of large momentum transfer exclusive nuclear processes. Rigorous results have been given by Lepage, Ji and myself[80] for the asymptotic properties of the deuteron form factor at large momentum transfer. The basic factorization is shown in Fig. 35. In the asymptotic $Q^2 \rightarrow \infty$ limit the deuteron distribution ampli-

48

tude, which controls large momentum transfer deuteron reactions, becomes fully
symmetric among the five possible color-singlet combinations of the six quarks.
One can also study the evolution of the "hidden color" components (orthogonal to
the np and ΔΔ degrees of freedom) from intermediate to large momentum transfer
scales; the results also give constraints on the nature of the nuclear force at short
distances in QCD.[81]

Of the five color-singlet representations of six quarks, only one corresponds
to the usual system of two color singlet baryonic clusters.[82] The exchange of a
virtual gluon in the deuteron at short distance inevitably produces Fock state
components where the three-quark clusters correspond to color octet nucleons
or isobars. Thus, in general, the deuteron wave function will have a complete
spectrum of "hidden-color" wave function components, although it is likely that
these states are important only at small internucleon separation.
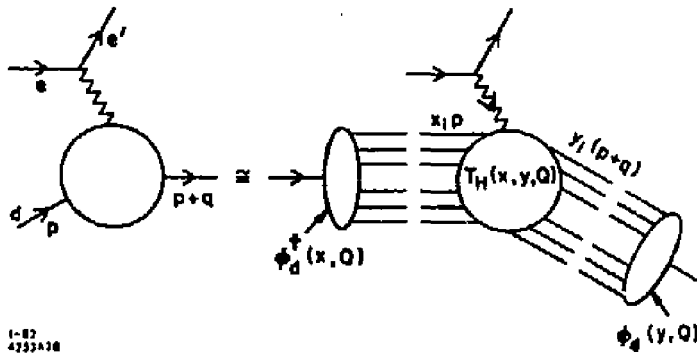
Fig. 35. Factorization of the deuteron form factor at large $Q^2$ in QCD.

Despite the complexity of the multicolor representations of nuclear wave
functions, the analysis[80] of the deuteron form factor at large momentum transfer
can be carried out in parallel with the nucleon case. Only the minimal six-quark
Fock state needs to be considered to leading order in $1/Q^2$. The deuteron form
factor can then be written as a convolution as in Fig. 35,

$$F_d(Q^2) = \int_0^1 [dx] \, [dy] \, \phi_d^\dagger(y,Q) \, T_H^{6q+\gamma^*-6q}(x,y,Q) \, \phi_d(x,Q) \,,$$

where the hard scattering amplitude scales as

$$T_H^{6q+\gamma^*\to 6q} = \left[\frac{\alpha_s(Q^2)}{Q^2}\right]^5 t(x,y)\ \left[1 + \mathcal{O}(\alpha_s(Q^2))\right]\ .$$

The anomalous dimensions $\gamma_n^d$ are calculated from the evolution equations for $\phi_d(x_i, Q)$ derived to leading order in QCD from pairwise gluon-exchange interactions: ($C_F = 4/3$, $C_d = -C_F/5$)

$$\prod_{k=1}^{6} x_k \left[\frac{\partial}{\partial\xi} + \frac{3C_F}{\beta}\right]\widetilde{\Phi}(x_i, Q) = -\frac{C_d}{\beta}\int_0^1 [dy]\ V(x_i, y_i)\bar{\Phi}(y_i, Q)\ .$$

Here we have defined

$$\Phi(x_i, Q) = \prod_{k=1}^{6} x_k \widetilde{\Phi}(x_i, Q)\ ,$$

and the evolution is in the variable

$$\xi(Q^2) = \frac{\beta}{4\pi}\int_{Q_0^2}^{Q^2}\frac{dk^2}{k^2}\alpha_s(k^2) \sim \ln\left(\frac{\ln\frac{Q^2}{\Lambda^2}}{\ln\frac{Q_0^2}{\Lambda^2}}\right)\ .$$

The kernel $V$ is computed to leading order in $\alpha_s(Q^2)$ from the sum of gluon interactions between quark pairs. The general matrix representations of $\gamma_n$ with bases $\left|\prod_{i=1}^{5} x_i^{m_i}\right\rangle$ is given in Ref. 81. The effective leading anomalous dimension $\gamma_0$, corresponding to the eigenfunction $\widetilde{\Phi}(x_i) = 1$, is $\gamma_0 = (6/5)(C_F/\beta)$.

To make more detailed and experimentally accessible predictions, we define the "reduced" nuclear form factor. This removes the effects of nucleon compositeness:[83]

$$f_d(Q^2) \equiv \frac{F_d(Q^2)}{F_N^2(Q^2/4)}\ .$$

The arguments for each of the nucleon form factors ($F_N$) is $Q^2/4$ since in the limit of zero binding energy each nucleon must change its momentum from $\sim p/2$ to $(p + q)/2$. This is illustrated in Fig. 36. Since the leading anomalous dimension of the nucleon distribution amplitude is $C_F/2\beta$, the QCD prediction for the asymptotic $Q^2$-behavior of $f_d(Q^2)$ is

$$f_d(Q^2) \sim \frac{\alpha_s(Q^2)}{Q^2}\left(\ln\frac{Q^2}{\Lambda^2}\right)^{-\frac{2}{5}\frac{C_F}{\beta}}\ ,$$

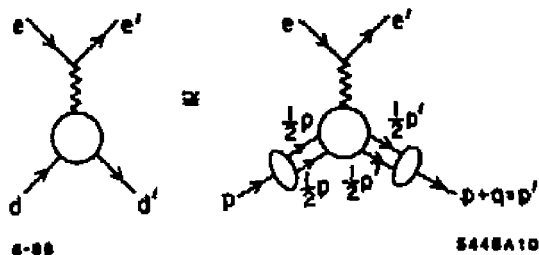where $-(2/5)(C_F/\beta) = -8/145$ for $n_f = 2$.

Fig. 36. Application of the reduced amplitude formalism to the deuteron form factor at large momentum transfer.

Although this QCD prediction is for asymptotic momentum transfer, it is interesting to compare it directly with the available high $Q^2$ data[84] (see Fig. 37). In general, one would expect corrections from higher twist effects (e.g., mass and $k_\perp$ smearing), higher particle number Fock states, higher order contributions in $\alpha_s(Q^2)$, as well as nonleading anomalous dimensions. However, the agreement of the data with simple $Q^2 f_d(Q^2) \sim const$ behavior for $Q^2 > 1/2$ GeV$^2$ implies that, unless there is a fortuitous cancellation, all of the scale-breaking effects are small, and the present QCD perturbative calculations are viable and applicable even in the nuclear physics domain. The lack of deviation from the QCD parameterization also suggests that the parameter $\Lambda$ is small. A comparison with a standard definition such as $\Lambda_{\overline{MS}}$ would require a calculation of next to leading effects. A more definitive check of QCD can be made by calculating the normalization of $f_d(Q^2)$ from $T_H$ and the evolution of the deuteron wave function to short distances. It is also important to confirm experimentally that the helicity $\lambda = \lambda' = 0$ form factor is indeed dominant.

Because of hidden color, the deuteron cannot be described solely in terms of standard nuclear physics degrees of freedom and, in principle, any physical or dynamical property of the deuteron is modified by the presence of such non-Abelian components. In particular, the standard "impulse approximation" form for the deuteron form factor

$$F_d(Q^2) = F_d^{body}(Q^2)\, F_N(Q^2)\,,$$

where $F_N$ is the on-shell nucleon form factor, cannot be precisely valid at any momentum transfer scale $Q^2 = -q^2 \neq 0$ because of hidden color compo-
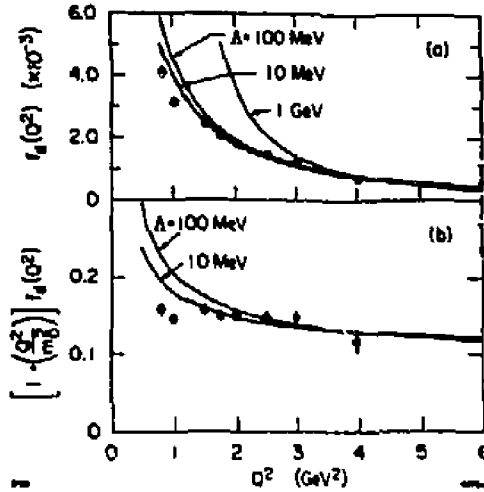
Fig. 37. (a) Comparison of the asymptotic QCD prediction for the reduced form factor with the SLAC/American University experiment using $F_N(Q^2) = [1 + (Q^2/0.71\,\text{GeV}^2)]^{-2}$. The normalization is fit at $Q^2 = 4$ GeV$^2$. (b) Comparison of the prediction $[1 + (Q^2/m_0^2)] f_d(Q^2) \propto (\ln Q^2)^{-1-(2/5)(C_F/\beta)}$ with data. The value $m_0^2 = 0.28$ GeV$^2$ is used. It is assumed that the helicity conserving form factor is dominant. The helicity-flip form factor is predicted to be suppressed by factors of $1/Q$ and may have an interference structure due to perturbative QCD contributions.

nents. More important, even if only the nucleon-nucleon component were important, the conventional factorization cannot be reliable for composite nucleons since the struck nucleon is necessarily off-shell[85] in the nuclear wave function: $|k'^2 - k^2| \sim \frac{1}{2}Q^2$. Thus, in general, one requires knowledge of the nucleon form factors $F_N(q^2, k^2, k'^2)$ for the case in which one or both nucleon legs are off-shell. In QCD such amplitudes have completely different dynamical dependence compared to the on-shell form factors.

Although on-shell factorization has been used extensively in nuclear physics as a starting point for the analysis of nuclear form factors,[86] its range of validity has never been seriously questioned. Certainly in the nonrelativistic domain where target recoil and off-shell effects can be neglected, the charge form factor of a composite system can be computed from the convolution of charge distributions. However, in the general situation, the struck nucleon must transfer a large fraction of its momentum to the spectator system, rendering the nucleon state off-shell. As

shown in Ref. 81, the region of validity of on-shell form factor factorization for the deuteron is very small:

$$Q^2 < 2 M_d \epsilon_d \ ,$$

i.e., $Q \lesssim 100$ MeV. However, in this region the nucleon form factor does not deviate significantly from unity, so the standard factorization is of doubtful utility. The reduced form factor result has general utility at any momentum scale. It is also important to confirm experimentally that the helicity $\lambda = \lambda' = 0$ form factor is indeed dominant.

The calculation of the normalization $T_H^{6q+\gamma^* \to 6q}$ to leading order in $\alpha_s(Q^2)$ will require the evaluation of over 300,000 Feynman diagrams involving five exchanged gluons. Fortunately this appears possible using the algebraic computer methods introduced by Farrar and Neri.[87] The method of setting the appropriate scale $\hat{Q}$ of $\alpha_s^5(\hat{Q}^2)$ in $T_H$ is given in Ref. 88.

The deuteron wave function which contributes to the asymptotic limit of the form factor is the totally antisymmetric wave function corresponding to the orbital Young symmetry given by [6] and isospin $(T)$+ spin $(S)$ Young symmetry given by {33}. The deuteron state with this symmetry is related to the $NN$, $\Delta\Delta$, and hidden color $(CC)$ physical bases, for both the $(TS) = (01)$ and $(10)$ cases, by the formula[89]

$$\psi_{[6]\{33\}} = \sqrt{\frac{1}{9}} \, \psi_{NN} + \sqrt{\frac{4}{45}} \, \psi_{\Delta\Delta} + \sqrt{\frac{4}{5}} \, \psi_{CC} \ .$$

Thus the physical deuteron state, which is mostly $\psi_{NN}$ at large distance, must evolve to the $\psi_{[6]\{33\}}$ state when the six-quark transverse separations $b_\perp^i \leq \mathcal{O}(1/Q) \to 0$. Since this state is 80% hidden color, the deuteron wave function cannot be described by the meson-nucleon isobar degrees of freedom in this domain. The fact that the six-quark color singlet state inevitably evolves in QCD to a dominantly hidden-color configuration at small transverse separation also has implications for the form of the nucleon-nucleon ($S_z = 0$) potential, which can be considered as one interaction component in a coupled scattering channel system. As the two nucleons approach each other, the system must do work in order to change the six-quark state to a dominantly hidden color configuration, i.e., QCD requires that the nucleon-nucleon potential must be repulsive at short distances (see Fig. 38).[90] The evolution equation for the six-quark system suggests that the distance where this change occurs is in the domain where $\alpha_s(Q^2)$ most strongly

varies. The general solutions of the evolution equation for multiquark systems is discussed in Ref. 81. Some of the solutions are orthogonal to the usual nuclear configurations which correspond to separated nucleons or isobars at large distances.
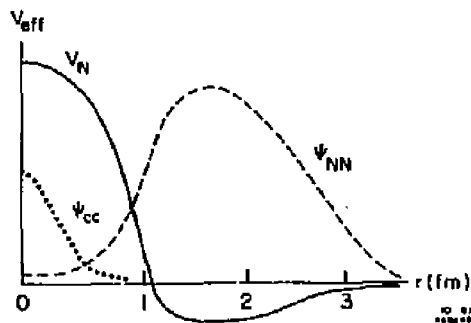


Fig. 38.    Schematic representation of the deuteron wave function in QCD indicating the presence of hidden color six-quark components at short distances.

The existence of hidden color degrees of freedom further illustrates the complexity of nuclear systems in QCD. It is conceivable that six-quark $d^*$ resonances corresponding to these new degrees of freedom may be found by careful searches of the $\gamma^* d \rightarrow \gamma d$ and $\gamma^* d \rightarrow \pi d$ channels.

## 11.    REDUCED NUCLEAR AMPLITUDES

One of the basic problems in the analysis of nuclear scattering amplitudes is how to consistently account for the effects of the underlying quark/gluon component structure of nucleons. Traditional methods based on the use of an effective nucleon/meson local Lagrangian field theory are not really applicable, giving the wrong dynamical dependence in virtually every kinematic variable for composite hadrons. The inclusion of *ad hoc* vertex form factors is unsatisfactory since one must model the off-shell dependence in each leg while retaining gauge invariance; such methods have little predictive power. On the other hand, the explicit evaluation of the multiquark hard-scattering amplitudes needed to predict the normalization and angular dependence for a nuclear process, even at leading order in $\alpha_s$ requires the consideration of millions of Feynman diagrams. Beyond leading

order one must include contributions of nonvalence Fock state wave functions, and a rapidly expanding number of radiative corrections and loop diagrams.

The reduced amplitude method,[83] although not an exact replacement for a full QCD calculation, provides a simple method for identifying the dynamical effects of nuclear substructure, consistent with covariance, QCD scaling laws and gauge invariance. The basic idea has already been introduced for the reduced deuteron form factor. More generally, if we neglect nuclear binding, then the light-cone nuclear wave function can be written as a cluster decomposition of collinear nucleons: $\psi_{q/A} = \psi_{N/A} \prod_N \Psi_{q/N}$ where each nucleon has $1/A$ of the nuclear momentum. A large momentum transfer nucleon amplitude then contains as a factor the probability amplitude for each nucleon to remain intact after absorbing $1/A$ of the respective nuclear momentum transfer. We can identify each probability amplitude with the respective nucleon form factor $F(\hat{t}_i = \frac{1}{A^2} t_A)$. Thus, for any exclusive nuclear scattering process, we define the reduced nuclear amplitude

$$m = \frac{M}{\prod_{i=1}^{A} F_N(\hat{t}_i)} \ .$$

The QCD scaling law for the reduced nuclear amplitude $m$ is then identical to that of nuclei with point-like nuclear components, e.g., the reduced nuclear form factors obey

$$f_A(Q^2) \equiv \frac{F_A(Q^2)}{\left[ F_N(Q^2/A^2) \right]^A} \sim \left[ \frac{1}{Q^2} \right]^{A-1} \ .$$

Comparisons with experiment and predictions for leading logarithmic corrections to this result are given in Ref. 83. In the case of photodisintegration (or electro-disintegration) of the deuteron one has

$$m_{\gamma d \to np} = \frac{M_{\gamma d \to np}}{F_n(t_n) F_p(t_p)} \sim \frac{1}{p_T} f(\theta_{cm}) \ ,$$

i.e., the same elementary scaling behavior as for $M_{\gamma M \to qq}$. Comparison with experiment is encouraging (see Fig. 39) showing that as was the case for $Q^2 f_d(Q^2)$, the perturbative QCD scaling regime begins at $Q^2 \gtrsim 1$ GeV$^2$. Detailed comparisons and a model for the angular dependence and the virtual photon-mass dependence of deuteron electrodisintegration are discussed in Ref. 83. Other potentially useful checks of QCD scaling of reduced amplitudes are

$$m_{pp \to d\pi^+} \sim p_T^{-2} \, f(t/s)$$

$$m_{pd \to H^3\pi^+} \sim p_T^{-4} \, f(t/s)$$

$$m_{\pi d \to \pi d} \sim p_T^{-4} \, f(t/s) \, .$$

It is also possible to use these QCD scaling laws for the reduced amplitude as a parametrization for the background for detecting possible new di-baryon resonance states. In each case, the incident and outgoing hadron and nuclear states are predicted to display color transparency, i.e., the absence of initial and final state interactions if they participate in a large momentum transfer exclusive reaction.
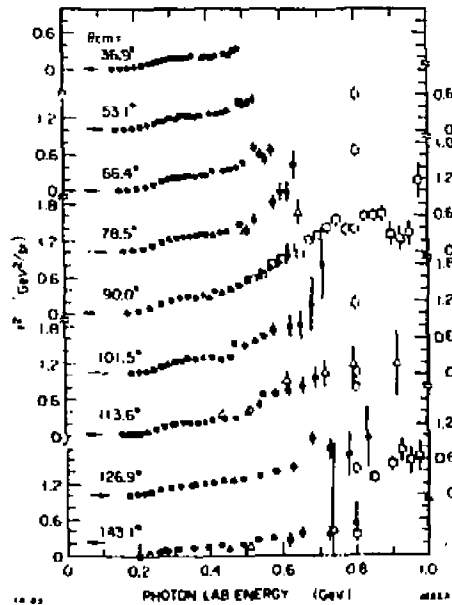


Fig. 39. Comparison of deuteron photodisintegration data with the scaling prediction which requires $f^2(\theta_{cm})$ to be independent of energy at large momentum transfer. The data are from H. Myers et al., Phys. Rev. **121**, 630 (1961); R. Ching and C. Schaerf, Phys. Rev. **141**, 1320 (1966); P. Dougan et al., Z. Phys. A **276**, 55 (1976).

## 12. HELICITY SELECTION RULE AND EXCLUSIVE CHARMONIUM DECAYS

One of the simplest predictions of perturbative QCD for exclusive processes is hadron helicity conservation: to leading order in $1/Q$, the total helicity of hadrons in the initial state must equal the total helicity of hadrons in the final state. This selection rule is independent of any photon or lepton spin appearing in the process. The result follows from (a) neglecting quark mass terms, (b) the vector coupling of gauge particles and (c) the dominance of valence Fock states with zero angular momentum projection.[91]

Hadron helicity conservation may be relevant to an interesting puzzle concerning the exclusive decays $J/\psi$ and $\psi' \to \rho\pi, K^*\overline{K}$ and possibly other Vector-Pseudoscalar (VP) combinations. One expects $J/\psi(\psi')$ to decay to hadrons via three gluons or, occasionally, via a single direct photon. In either case, the decay proceeds via $|\Psi(0)|^2$, where $\Psi(0)$ is the wave function at the origin in the non-relativistic quark model for $c\bar{c}$. Thus, it is reasonable to expect on the basis of perturbative QCD, that for any final hadronic state $h$:

$$Q_h \equiv \frac{B(\psi' \to h)}{B(J/\psi \to h)} \cong \frac{B(\psi' \to e^+e^-)}{B(J/\psi \to e^+e^-)} = 0.135 \pm 0.023 \ .$$

Usually this is true, as is well documented in Ref. 92, for $p\bar{p}\pi^0$, $2\pi^+2\pi^-\pi^0$, $\pi^+\pi^-\omega$ and $3\pi^+3\pi^-\pi^0$, hadronic channels. The startling exceptions occur for $\rho\pi$ and $K^*\overline{K}$ where the present experimental limits[92] are

$$Q_{\rho\pi} < 0.0063 \quad \text{and} \quad Q_{K^*\overline{K}} < 0.0027 \ .$$

Recently San Fu Tuan, Peter Lepage and I[93] have proposed an explanation of the puzzle by assuming (a) the general validity of the perturbative QCD theorem that total hadron helicity is conserved in high momentum transfer exclusive processes, but supplemented by (b) violation of the QCD theorem when the $J/\psi$ decay to hadrons via three hard gluons is modulated by the gluons forming an intermediate gluonium state $\mathcal{O}$ before transition to hadrons. In essence, the model of Hou and Soni[94] takes over in this latter stage.

Since the vector state $V$ has to be produced with helicity $\lambda = \pm 1$, the $VP$ decays should be suppressed by a factor $1/s$ in the rate. The $\psi'$ seems to respect this rule. The $J/\psi$ does *not*, and that is the mystery. Put in more quantitative terms, we expect on the basis of perturbative QCD[91]

$$Q_{\rho\pi} \equiv \frac{B(\psi' \to \rho\pi)}{B(J/\psi \to \rho\pi)} \sim [M_{J/\psi}/M_{\psi'}]^6 \; ,$$

assuming quark helicity is conserved in strong interactions. This includes a form factor suppression proportional to $[M_{J/\psi}/M_{\psi'}]^4$. This suppression is not nearly large enough, though, to account for the data.

One can question the validity of the QCD helicity conservation theorem at the charmonium mass scale. Helicity conservation has received important confirmation in $J/\psi \to p\bar{p}$ where the angular distribution is known experimentally to follow $[1 + \cos^2 \theta]$ rather than $\sin^2 \theta$ for helicity flip. The $\psi'$ decays clearly respect hadron helicity conservation. It is difficult to understand how the $J/\psi$ could violate this rule since the $J/\psi$ and $\psi'$ masses are so close. Corrections from quark mass terms, soft gluon corrections and finite energy corrections would not be expected to lead to large $J/\psi$ differences. It is hard to imagine anything other than a resonant or interference effect that could account for such dramatic energy dependence.

A relevant violation of the QCD theorem which does have significance to this problem, is the recognition that the theorem is built on the underlying assumption of short-range "point-like" interactions amongst the constituents throughout. For instance, $J/\psi(c\bar{c}) \to 3g$ has a short-range $\cong 1/m_c$ associated with the short time scale of interaction. If, however, subsequently the three gluons were to resonate forming a gluonium state $\mathcal{O}$ which has large transverse size $\cong 1/M_H$ covering an extended (long) time period, then the theorem is invalid. Note that even if the gluonium state $\mathcal{O}$ has large mass, close to $M_{J/\psi}$, its size could still be the standard hadronic scale of 1 fm, just as the case for the $D$-mesons and $B$-mesons.

We have thus proposed, following Hou and Soni, that the enhancement of $J/\psi \to K^*\overline{K}$ and $J/\psi \to \rho\pi$ decay modes is caused by a quantum mechanical mixing of the $J/\psi$ with a $J^{PC} = 1^{--}$ vector gluonium state $\mathcal{O}$ which causes the breakdown of the QCD helicity theorem. The decay width for $J/\psi \to \rho\pi(K^*\overline{K})$ via the sequence $J/\psi \to \mathcal{O} \to \rho\pi(K^*\overline{K})$ must be substantially larger than the decay width for the (nonpole) continuum process $J/\psi \to 3$ gluons $\to \rho\pi(K^*\overline{K})$. In the other channels (such as $p\bar{p}, p\bar{p}\pi^0, 2\pi^+2\pi^-\pi^0$, etc.), the branching ratios of the $\mathcal{O}$ must be so small that the continuum contribution governed by the QCD theorem dominates over that of the $\mathcal{O}$ pole. For the case of the $\psi'$ the contribution of the

$\mathcal{O}$ pole must always be inappreciable in comparison with the continuum process where the QCD theorem holds. The experimental limits on $Q_{\rho\pi}$ and $Q_{K^*\overline{K}}$ are now substantially more stringent than when Hou and Soni made their estimates of $M_{\mathcal{O}}$, $\Gamma_{\mathcal{O}\to\rho\pi}$ and $\Gamma_{\mathcal{O}\to K^*\overline{K}}$ in 1982.

It is interesting, indeed, that the existence of such a gluonium state $\mathcal{O}$ was first postulated by Freund and Nambu[95] based on $OZI$ dynamics soon after the discovery of the $J/\psi$ and $\psi'$ mesons. In fact, Freund and Nambu predicted that the $\mathcal{O}$ would decay copiously precisely into $\rho\pi$ and $K^*\overline{K}$ with severe suppression of decays into other modes like $e^+e^-$ as required for the solution of the puzzle.

Final states $h$ which can proceed only through the intermediate gluonium state satisfy the ratio:

$$Q_h = \frac{B(\psi' \to e^+e^-)}{B(J/\psi \to e^+e^-)} \frac{(M_{J/\psi} - M_{\mathcal{O}})^2 + \frac{1}{4}\Gamma_{\mathcal{O}}^2}{(M_{\psi'} - M_{\mathcal{O}})^2 + \frac{1}{4}\Gamma_{\mathcal{O}}^2} .$$

We have assumed that the coupling of the $J/\psi$ and $\psi'$ to the gluonium state scales as the $e^+e^-$ coupling. The value of $Q_h$ is small if the $\mathcal{O}$ is close in mass to the $J/\psi$. Thus we require

$$(M_{J/\psi} - M_{\mathcal{O}})^2 + \frac{1}{4}\Gamma_{\mathcal{O}}^2 \lesssim 2.6\, Q_h \text{ GeV}^2 .$$

The experimental limit for $Q_{K^*\overline{K}}$ then implies

$$\left[(M_{J/\psi} - M_{\mathcal{O}})^2 + \frac{1}{4}\Gamma_{\mathcal{O}}^2\right]^{1/2} \lesssim 80 \text{ MeV} .$$

This implies $|M_{J/\psi} - M_{\mathcal{O}}| < 80$ MeV and $\Gamma_{\mathcal{O}} < 160$ MeV. Typical allowed values are

$$M_{\mathcal{O}} = 3.0 \text{ GeV}, \quad \Gamma_{\mathcal{O}} = 140 \text{ MeV}$$

or

$$M_{\mathcal{O}} = 3.15 \text{ GeV}, \quad \Gamma_{\mathcal{O}} = 140 \text{ MeV} .$$

Notice that the gluonium state could be either lighter or heavier than the $J/\psi$. The branching ratio of the $\mathcal{O}$ into a given channel must exceed that of the $J/\psi$.

It is not necessarily obvious that a $J^{PC} = 1^{--}$ gluonium state with these parameters would necessarily have been found in experiments to date. One must remember that, although $\mathcal{O} \to \rho\pi$ and $\mathcal{O} \to K^*\overline{K}$ are important modes of decay, at a mass of order 3.1 GeV many other modes (all be it less important) are available. Hence, a total width $\Gamma_{\mathcal{O}} \cong 100$ to 150 MeV is quite conceivable. Because of

the proximity of $M_{\mathcal{O}}$ to $M_{J/\psi}$, the most important signatures for an $\mathcal{O}$ search via exclusive modes $J/\psi \to K^*\overline{K}h$, $J/\psi \to \rho\pi h$; $h = \pi\pi, \eta, \eta'$, are no longer available by phase-space considerations. However, the search could still be carried out using $\psi' \to K^*\overline{K}h$, $\psi' \to \rho\pi h$; with $h = \pi\pi$, and $\eta$. Another way to search for $\mathcal{O}$ in particular, and the three-gluon bound states in general, is via the inclusive reaction $\psi' \to (\pi\pi) + X$, where the $\pi\pi$ pair is an isosinglet. The three-gluon bound states such as $\mathcal{O}$ should show up as peaks in the missing mass (i.e., mass of $X$) distribution.

Perhaps the most direct way to search for the $\mathcal{O}$ is to scan $\overline{p}p$ or $e^+e^-$ annihilation at $\sqrt{s}$ within $\sim 100$ MeV of the $J/\psi$, triggering on vector/pseudoscalar decays such as $\pi\rho$ or $\overline{K}K^*$.

The fact that the $\rho\pi$ and $K^*\overline{K}$ channels are strongly suppressed in $\psi'$ decays but not in $J/\psi$ decays clearly implies dynamics beyond the standard charmonium analysis. As we have shown, the hypothesis of a three-gluon state $\mathcal{O}$ with mass within $\cong 100$ MeV of the $J/\psi$ mass provides a natural, perhaps even compelling, explanation of this anomaly. If this description is correct, then the $\psi'$ and $J/\psi$ hadronic decays are not only confirming hadron helicity conservation (at the $\psi'$ momentum scale) but are also providing a signal for bound gluonic matter in QCD.

## 13.  CONCLUSIONS

Quantum Chromodynamics (QCD) is a remarkably interesting theory. As we have seen in these lectures, many novel and unexpected phenomena appear when QCD processes are studied in the nuclear enviroment. We now are beginning to confront the nonperturbative nature of the theory and effects which are important in the few GeV domain. The hadroproduction of charmed hadrons and charmonium plays an important role in these studies, and it is essential that discrepancies between experiments be resolved.

There has been considerable progress understanding the structure of the hadrons and their interactions from first principles in QCD. Lattice gauge theory and QCD sum rules are providing beautiful constraints on the basic shape of the distribution amplitudes of the mesons and baryons. A new method, discretized light-cone quantization, has been tested successfully for QCD in one-space and one-time dimensions and should soon yield detailed information on physical light-cone wave functions.

The recent work of Dziembowski and Mankiewicz[38] provides a convenient relativistic model for hadronic wave functions consistent with the known constraints. Their work provides the starting point for a consistent description of exclusive amplitudes such as form factors from low to high momentum transfer. The controversy concerning the range of validity of perturbative QCD predictions for exclusive amplitudes has thus been largely resolved. Where clear tests can be made, such as two-photon processes and the hadron form factors, the perturbative QCD predictions appear correct in scaling behavior, helicity structure and absolute normalization. Most interesting, there is now evidence for the remarkable color transparency phenomenon predicted by perturbative QCD for quasi-elastic scattering within a nucleus. Further experiments, particularly quasi-elastic lepton-proton scattering are crucial.[96]

One of the most serious challenges to the validity of QCD are the pseudo-scalar vector decays of the $J/\psi$. We have shown that this puzzle can be resolved if a gluonium state exists with mass near 3 GeV/c. I have also discussed a possible explanation for the strong spin correlations in proton-proton elastic scattering and the reversal of color transparency in terms of a novel type of high mass di-baryon resonance. For each case, the $J/\psi$ anomaly, the structure in $A_{NN}$, and the change in transparency of the nucleus, one can attribute the breakdown of the perturbation prediction to a threshold phenomena which requires that the full large scale structure of the hadrons is involved. It is important to identify explicitly the inelastic channels responsible for the new threshold in $pp$ scattering near $\sqrt{s} = 5$ GeV—perhaps open charm states. A key tool in this analysis is the use of color transparency in nuclei to filter out large and short distance phenomena.

I have also discussed the role of the formation zone and the target length condition in understanding the absence of inelastic nuclear effects in the propagation of high energy quarks and gluons in nuclear matter. Conversely, coalescence of the produced particles with co-moving spectators was shown to produce a number of unexpected effects such as enhancement of charmed hadron production but the suppression of charmonium production in nuclear collisions.

Finally, I have discussed applications of QCD to nuclear amplitudes and to the basic structure of the nucleus itself. I have also noted areas of potential conflict between QCD and more conventional approaches to nuclear interactions, e.g., Dirac phenomenology factorization of on-shell nucleon form factors, and the

breakdown of conventional Glauber theory due to color transparency in exclusive reactions, and formation zone phenomenology in inclusive reactions.

## ACKNOWLEDGMENTS

## REFERENCES

1. Ashman, J. et al., CERN preprint CERN-EP/87-230.

2. Brodsky, S. J., Ellis, J. and Karliner, M., SLAC-PUB-4519, (1988).

3. Lepage, G. P. and Brodsky, S. J., Phys. Rev. **D22**, 2157 (1980); Lepage, G. P., Brodsky, S. J., Huang, T. and Mackenzie, P. B., CLNS-82/522, published in the Proc. of the Banff Summer Institute, 1981.

4. Brodsky, S. J., Frishman, Y., Lepage, G. P. and Sachrajda, C., Phys. Lett. **91B**, 239 (1980).

5. Brodsky, S. J., SLAC-PUB-4342, in the Proc. of the VIIIth Nuclear and Particle Physics Summer School, Launceston, Australia, 1987.

6. Chernyak, V. L., Ogloblin, A. A. and Zhitnitsky, I. R., Novosibirsk preprints 87-135, 136, and Refs. therein.

7. Pauli, H. C. and Brodsky, S. J., Phys. Rev. **D32**, 1993 (1985); Phys. Rev. **D32**, 2001 (1985).

8. Brodsky, S. J., Bodwin, G. T. and Lepage, G. P., in the Proc. of the Volendam Multipart. Dyn. Conf., 1982, p. 841; Proc. of the Banff Summer Inst., 1981, p. 513. This effect is related to the formation zone principle of L. Landau and I. Pomeranchuk, Dok. Akademii Nauk SSSR **92**, 535, 735 (1953).

9. Bordalo, P. et al., CERN EP/87-67 and 68 (1987); Betev, B. et al., Z. Phys. **C28**, 9, 15 (1985).

10. For further references and a phenomenological analysis, see P. Chiappetta and H. J. Pirner, Nucl. Phys. **B291**, 765 (1987).

11. Brodsky, S. J., Gunion, J. F. and Soper, D., Phys. Rev. D36, 2710, 1987.

12. Biagi, S. F. et al., Z. Phys. C28, 175 (1985).

13. Brodsky, S. J. and Mueller, A. H., NSF-ITP-88-22.

14. See the discussions of J. D. Bjorken and A. H. Mueller, Proc. of the NATO Research Workshop on Hard Hadronic Processes, St. Croix (1987).

15. Mueller, A. H., Ref. 14.

16. Mueller, A. H., Proc. of the Moriond Conf., 1982; Brodsky, S. J., XIII Int. Symp. on Multiparticle Dynamics, Volendam, 1982. See also, Bertsch. G., Brodsky, S. J., Goldhaber, A. S. and Gunion, J. F., Phys. Rev. Lett. 47, 297 (1981).

17. Heppelmann, S. et al., DPF Meeting, Salt Lake City, 1987; Carroll, A. S. et al., this institute, and BNL preprint, 1988.

18. Brodsky, S. J. and de Teramond, G., SLAC-PUB 4504 (1987), to be published in Phys. Rev. Lett.

19. Court, G. R. et al., Phys. Rev. Lett. 57, 507 (1986); Bhatia, T. S. et al., Phys. Rev. Lett. 49, 1135 (1982); Crosbie, E. A. et al., Phys. Rev. D23, 600 (1981); Lin, A. et al., Phys. Lett. 74B, 273 (1978); Crabb, D. G. et al., Phys. Rev. Lett. 41, 1257 (1978); O'Fallon, J. R. et al., Phys. Rev. Lett. 39, 733 (1977). For a review, see A. D Krisch, UM-HE 86-39 (1987).

20. Brodsky, S. J., SLAC-PUB 4451, to be published in Proc. of the 4th LEAR Workshop, Villars-sur Ollon, Switzerland (1987).

21. Brodsky, S. J. and Mueller, A. H., to be published.

22. An analysis of Z-graph suppression for composite systems will be given by S. J. Brodsky and T. Jaroszewicz (in progress). See also, M. Blesynski and T. Jaroszewski, UCLA preprint, 1987.

23. Matsui, T. and Satz, H., Phys. Lett. B178, 416 (1987).

24. Sommerfeld, S., Atombau and Spektrallinen (Vieweg, Braunschweig, 1939).

25. Brodsky, S. J., Kopp, G. and Zerwas, P., Phys. Rev. Lett. 58, 443 (1987).

26. Bordalo, P. et al., CERN EP/87 67 and 68 (1987).

27. For a recent review and further theoretical references, see E. L. Berger and F. Coester, ANL-HEP-PR-87-13 (1987).

28. Aubert, J. J. et al., Phys. Lett. 123B, 275 (1983). For recent reviews, see E. L. Berger, ANL-HEP-PR-87-45 and E. L. Berger and F. Coester, ANL HEP-PR-87-13 (to be published in Ann. Rev. of Nucl. Part. Sci.).

29. H.G. Fischer, presented at the Leipzig Conference, 1984.

30. Alexander, G., Gotsman, E. and Maor, U., Phys. Lett. **161B**, 384 (1985).

31. Brodsky, S. J. and Soldate, M., unpublished.

32. Brodsky, S. J. and Farrar, G. R., Phys. Rev. Lett. **31**, 1153 (1973); Phys. Rev. **D11**, 1309 (1975).

33. Brodsky, S. J. and Lepage, G. P., Phys. Rev. **D23**, 1152 (1981); Brodsky, S. J., Lepage, G. P. and Zaidi, S. A. A., Phys. Rev. **D23**, 1152 (1981).

34. Brodsky, S. J. and Lepage, G. P., Phys. Rev. **D24**, 2848 (1981).

35. Burkert, V. D., CEBAF-PR-87-006.

36. Chernyak, V. L. and Zhitnitskii, A. R., Phys. Rep. **112**, 173 (1984). See also, Xiao Duang Xiang, Wang Xin-Nian and Huang Tao, BIHEP TH-84, 23 and 29 (1984).

37. King, I. D. and Sachrajda, C. T., SHEP 85/86 15 (1986), p. 36.

38. Dziembowski, Z. and Mankiewicz, L., Warsaw University preprint (1986). Dziembowski, Z., Phys. Rev. **D37**, 768, 778 (1988).

39. Brodsky, S. J. and Chertok, B. T., Phys. Rev. Lett. **37**, 269 (1976); Phys. Rev. **D114**, 3003 (1976).

40. Jacob, O. C. and Kisslinger, L. S., Phys. Rev. Lett. **56**, 225 (1986).

41. Isgur, N. and Llewellyn Smith, C. H., Phys. Rev. Lett. **52**, 1080 (1984).

42. Ji, C. R., Sill, A. F. and Lombard Nelsen, R. M., SLAC PUB 4068 (1986).

43. Arnold, R. G. et al., SLAC PUB 3810 (1986).

44. Gari, M. and Stefanis, N., Phys. Lett. **B175**, 462 (1986); Gari, M. and Stefanis, N., preprint RUB TPH 86 21 (1986).

45. Farrar, G. R., presented to the Workshop on Quantum Chromodynamics at Santa Barbara, 1988.

46. Boyer, J. et al., Phys. Rev. Lett. **56**, 207 (1986); Aihara, H. et al., Phys. Rev. Lett. **57**, 404 (1986).

47. Mueller, A. H., Phys. Rep. **73**, 237 (1981). See also, Kanwal, S. S., Phys. Lett. 294 (1984).

48. Sen, A., Phys. Rev. **D24**, 3281 (1981).

49. Brodsky, S. J. and Lepage, G. P., Phys. Rev. **D24**, 1808 (1981). The next to leading order evaluation of $T_H$ for these processes is given by B. Nezic. Ph.D. Thesis, Cornell Univ. (1985).

50. The spectrum of Yukawa theory is calculated in the usual Fock space by Brooks, E. D. and Frautschi, S. C., Z. Phys. **C23**, 263 (1984).

51. Dirac, P. A. M., Rev. Mod. Phys. **21**, 392 (1949). Further references to light-cone quantization are given in Ref. 53.

52. See, Brodsky, S. J., and Drell, S. D., Phys. Rev. **D22**, 2236 (1980), and references therein.

53. Eller, T., Pauli, H. C. and Brodsky, S. J., Phys. Rev. **D35**, 1493 (1987).

54. For a discussion of renormalization in light-cone perturbation theory see Brodsky, S. J., Roskies, R. and Suaya, R., Phys. Rev. **D8**, 4574 (1974), and also Ref. 3.

55. Bergknoff, H., Nucl. Phys. **B122**, 215 (1977).

56. McCartor, G., Z. Phys. **C36**, 329 (1987), and to be published.

57. Crewther, D. P. and Hamer, C. J., Nucl. Phys. **B170**, 353 (1980).

58. Harindranath, A. and Vary, J. P., Phys. Rev. **D36**, 1141 (1987).

59. Hornbostel, K., to be published.

60. Hamer, C. J., Nucl. Phys. **B195**, 503 (1981).

61. Frishman, Y. and Sonnenschein, J., Nucl. Phys. **B294**, 801 (1987), and preprint WIS-87/65-PH.

62. Tang, A., in preparation.

63. Klabucar, D. and Pauli, H. C., MPI H-1988-V4 (1988). This paper gives a compendium of results on the quantization of gauge theories in DLCQ and early references.

64. Brodsky, S. J., Carlson, C. E. and Lipkin, H. J., Phys. Rev. **D20**, 2278 (1979); Farrar, G. R., Gottlieb, S., Sivers, D. and Thomas, G., Phys. Rev. **D20**, 202 (1979).

65. For other attempts to explain the spin correlation data see, Avilez, C., Cocho, G. and Moreno, M., Phys. Rev. **D24**, 634 (1981); Farrar, G. R., Phys. Rev. Lett. **56**, 1643 (1986), ERRATUM—ibid. **56**, 2771 (1986); Lipkin, H. J., Nature **324**, 14 (1986); Troshin, S. M., Tyurin, N. E., JETP Lett. **44**, 149 (1986) [Pisma Zh. Eksp. Teor. Fiz. **44**, 117 (1986)]; Preparata, Soffer, Phys. Lett. **180B**, 281 (1986); Goloskokov, S. V., Kuleshov, S. P. and Seljugin, O. V., Proc. of the VII Int. Symposium on High Energy Spin Physics, Protvino (1986); Bourrely, C. and Soffer, J., Phys. Rev. **D35**, 145 (1987).

66. Lepage, G. P. and Brodsky, S. J., Phys. Rev. **D22**, 2157 (1980); Brodsky, S. J., Frishman, Y., Lepage, G. P. and Sachrajda, C., Phys. Lett. **94B**, 245 (1980); Duncan, A. and Mueller, A. H., Phys. Lett. **90B**, 159 (1980); Efremov, A. V. and Radyushkin, A. V., Phys. Lett. **94B**, 245 (1980); Mueller, A. H., Phys. Rep. **73**, 237 (1981); Chernyak, V. L. and Zhitnitskii, A. R., Phys. Rep. **112**, 173 (1984).

67. Brodsky, S. J. and Farrar, G. R., Phys. Rev. Lett. **31**, 1153 (1973); Matveev, V., Muradyan, R. and Tavkhelidze, A., Nuovo Cimento Lett. **7**, 719 (1973).

68. Brodsky, S. J. and Lepage, G. P., Phys. Rev. **D24**, 2848 (1981).

69. Blazey, G. C. et al., Phys. Rev. Lett. **55**, 1820 (1985); Blazey, G. C., Ph.D. Thesis, University of Minnesota (1987); Baller, B. R., Ph.D. Thesis, University of Minnesota (1987); Barton, D. S. et al., J. de Phys. **46**, C2, Supp. 2 (1985). For a review see, Sivers, D., Brodsky, S. J. and Blankenbecler, R., Phys. Rep. **23C**, 1 (1976).

70. There are five different combinations of six quarks which yield a color singlet B=2 state. It is expected that these QCD degrees of freedom should be expressed as B=2 resonances. See, e.g., S. J. Brodsky and C. R. Ji, Phys. Rev. **D34**, 1460 (1986).

71. For other examples of threshold enhancements in QCD see, S. J. Brodsky, J. F. Gunion and D. E. Soper, Phys. Rev. **D36**, 2710 (1987); S. J. Brodsky, G. Kopp and P. M. Zerwas, Phys. Rev. Lett. **58**, 443 (1987). Resonances are often associated with the onset of a new threshold. For a discussion see, D. Bugg, Presented at the IV LEAR Workshop, Villars-Sur-Ollon, Switzerland, Sept. 6-13, 1987.

72. Gunion, J. F., Blankenbecler, R. and Brodsky, S. J., Phys. Rev. **D6**, 2652 (1972).

73. With the above normalization, the unpolarized $pp$ elastic cross section is $d\sigma/dt = \Sigma_{i=1,2,...5} \mid \phi_i^2 \mid /(128\pi s p_{cm}^2)$.

74. Ralston, J. P. and Pire, B., Phys. Rev. Lett. **57**, 2330 (1986).

75. At low momentum transfers one expects the presence of both helicity-conserving and helicity nonconserving pomeron amplitudes. Preliminary calculations indicate that the data for $A_N$ at $p_{lab} = 11.75$ GeV/c can be understood over the full angular range in these terms. The large value of $A_N = 24 \pm 8\%$ at $p_{lab} = 28$ GeV/c and $p_T^2 = 6.5$ GeV$^2$ remains an open problem. See, Cameron, P. R. et al., Phys. Rev. **D32**, 3070 (1985).

76. Abe, K. et al., Phys. Rev. **D12**, 1 (1975), and references therein. The high energy data for $d\sigma/dt$ at $\theta_{cm} = \pi/2$ are from Akerlof, C. W. et al., Phys. Rev. **159**, 1138 (1967); Cocconi, G. et al., Phys. Rev. Lett. **11**, 499 (1963); Allaby, J. V. et al., Phys. Lett. **23**, 389 (1966).

77. Auer, I. P. et al., Phys. Rev. Lett. **52**, 808 (1984). Comparison with the low energy data for $A_{LL}$ at $\theta_{cm} = \pi/2$ suggests that the resonant amplitude below $p_{lab} = 5.5$ GeV/c has more structure than the single resonance form adopted here. See Auer, I. P. et al., Phys. Rev. Lett. **48**, 1150 (1982).

78. Hendry, A. W., Phys. Rev. **D10**, 2300 (1974); Jahren, N. and Hiller, J., University of Minnesota preprint, 1987.

79. The neutral strange inclusive $pp$ cross section measured at $p_{lab} = 5.5$ GeV/c is $0.45 \pm 0.04$ mb. Alexander, G. et al., Phys. Rev. **154**, 1284 (1967).

80. Ji, C.-R. and Brodsky, S. J., Phys. Rev. **D34**, 1460; **D33**, 1951; **D33**, 1406; **D33**, 2653 (1986); Phys. Rev. Lett. **55**, 2257 (1985).

81. Brodsky, S. J., Ji, C.-R. and Lepage, G. P., Phys. Rev. Lett. **51**, 83 (1983).

82. See, e.g., V. Matveev and P. Sorba, Nuovo Cimento Lett. **20**, 435 (1977).

83. Brodsky, S. J. and Hiller, J. R., Phys. Rev. **C28**, 475 (1983); Brodsky, S. J. and Chertok, B. T., Phys. Rev. Lett. **37**, 269 (1976), Phys. Rev. **D14**, 3003 (1976); Brodsky, S. J., Proc. of the International Conference on Few Body Problems in Nuclear and Particle Physics, Laval University, Quebec, 1974.

84. Mestayer, M. D., SLAC Report 214 (1978); Martin, F. et al., Phys. Rev. Lett. **38**, 1320 (1977); Schultz, W. P. et al., Phys. Rev. Lett. **38**, 259 (1977); Arnold, R. G. et al., Phys. Rev. Lett. **40**, 1429 (1978) and SLAC-PUB-2373 (1979); Chertok, B. T., Day, D. et al., Phys. Rev. Lett. **43**, 1143 (1979). Summaries of the data for nucleon and nuclear form factors at large $Q^2$ are given in B. T. Chertok, Progress in Particle and Nuclear Physics, Proc. of the International School of Nuclear Physics, 5th Course, Erice, 1978, and Proc. of the XVI Rencontre de Moriond, Les Arcs, Savoie, France, 1981.

85. For a general discussion of off-shell nucleon form factors, Bincer, A. M., Phys. Rev. **118**, 855 (1960).

86. Gurvitz, S. A., Phys. Rev. **C22**, 725 (1980). Meson exchange current contributions take the form of the reduced form factor. See, R. Blankenbecler and Gunion, J. F., Phys. Rev. **D4**, 718 (1971).

87. Farrar, G. R. and Neri, F., Phys. Lett. **130B**, 109 (1983).

88. Brodsky, S. J., Lepage, G. P. and Mackenzie, P. B., Phys. Rev. **D28**, 228 (1983).

89. Harvey, M., Nucl. Phys. **A352**, 301 (1981) and **A352**, 326 (1981).

90. Similar considerations for nonrelativistic systems are given in Faessler, A. et al., Nucl. Phys. **A402**, 555 (1983); Furui, S. and Faessler, A., Nucl. Phys. **A397**, 413 (1983).

91. Brodsky, S. J. and Lepage, G. P., Phys. Rev. **D24**, 2848 (1981).

92. Franklin, M. E. B., Ph.D. Thesis (1982), SLAC-254, UC-34d; Franklin, M. E. B. et al., Phys. Rev. Lett. **51**, 963 (1983); Trilling, G., Proc. of the 21st Int. Conf. on High Energy Physics, Paris, July 26-31, 1982; E. Bloom, ibid.

93. Brodsky, S. J., Lepage, G. P. and San Fu Tuan, Phys. Rev. Lett. **59**, 621 (1987).

94. Hou, Wei Shou and Soni, A., Phys. Rev. Lett. **50**, 569 (1983).

95. Freund, P. G. O. and Nambu, Y., Phys. Rev. Lett. **34**, 1645 (1975).

96. See, e.g., the report of R. Milner to this school.

# DISCLAIMER